AN ANISOTROPIC FINITE ELEMENT METHOD
ON POLYHEDRAL DOMAINS:
INTERPOLATION ERROR ANALYSIS

HENGGUANG LI

ABSTRACT. On a polyhedral domain $\Omega \subset \mathbb{R}^3$, consider the Poisson equation with the Dirichlet boundary condition. For singular solutions from the non-smoothness of the domain boundary, we propose new anisotropic mesh refinement algorithms to improve the convergence of finite element approximation. The proposed algorithm is simple, explicit, and requires less geometric conditions on the mesh and on the domain. Then, we develop interpolation error estimates in suitable weighted spaces for the anisotropic mesh, especially for the tetrahedra violating the maximum angle condition. These estimates can be used to design optimal finite element methods approximating singular solutions. We report numerical test results to validate the method.

1. INTRODUCTION

Let $\Omega \subset \mathbb{R}^3$ be a bounded polyhedral domain. Consider the Poisson equation with the Dirichlet boundary condition,

$$(1) \qquad -\Delta u = f \quad \text{in} \quad \Omega, \qquad u = 0 \quad \text{on} \quad \partial\Omega.$$

The regularity of the solution is determined by the smoothness of the boundary $\partial\Omega$ and the smoothness of the given data f. For example, when the domain has a smooth boundary, the solution continuously depends on the given data f in Sobolev spaces with the full regularity estimate [23, 32]

$$(2) \qquad \|u\|_{H^{m+1}(\Omega)} \leq C\|f\|_{H^{m-1}(\Omega)}, \qquad m \geq 0.$$

On domains with a non-smooth boundary, equation (1) usually possesses solutions with singularities near the non-smooth points, and therefore the estimate in (2) no longer holds, even when f is smooth. The lack of regularity in the solution can cause severe convergence issues in the numerical approximations [18, 20, 39].

Addressing critical problems both in theory and in practice, various finite element methods (FEMs) approximating such singular solutions have been studied. Intuitively, the accuracy of the numerical solution can be improved by increasing the mesh density near the singularity of the solution. For elliptic boundary value problems in two-dimensional (2D) polygonal domains, this idea has led to effective FEMs based on local mesh grading algorithms, in which the numerical approximation of singular solutions achieves the optimal convergence rate. See [1, 8, 12, 15, 31, 36, 37] and the references therein. The validation of these methods highly depends on the

regularity estimate of the singular solution in special weighted Sobolev spaces (e.g., [10, 21, 26, 27, 29, 34, 35]), which itself is an active research topic in mathematical analysis.

For a three-dimensional (3D) polyhedral domain Ω, the solution is featured with different types of singularities: the vertex (conical) singularity and the (anisotropic) edge singularity. Thus, an anisotropic mesh is in general expected for a better finite element approximation. The combination of different types of singularities, together with the complexity in the 3D geometry, makes the development of optimal FEMs for equation (1) a more technically challenging task. Existing algorithms on polyhedral domains usually require restrictive geometric conditions on the mesh and on the domain. Some relevant results are as follows. The mesh in [2, 25, 33] is based on the method of dyadic partitioning. These meshes are isotropic and optimal only for weaker singular solutions. The mesh in [1, 3–5] is based on a coordinate transformation from a quasi-uniform mesh. It is anisotropic along the edges and requires confining angle conditions for the simplex. The mesh in [9, 11] is also anisotropic and leads to optimal convergence rate. The algorithm, however, requires extra steps for prism refinements to maintain the angle condition in the simplex. There are also tensor-product anisotropic meshes based on 2D graded meshes [6, 38] that are usually effective on a domain with simple geometry.

The aim of this paper is twofold. First, we propose new anisotropic mesh refinement algorithms (Algorithm 3.2) for the finite element approximation of singular solutions in equation (1). These graded refinements are simple, explicit, and determined by a set of parameters associated to the singular set (vertices and edges) of the domain. Meanwhile, with less geometric requirements on the simplex and on the domain, these algorithms are defined recursively based on direct decomposition of tetrahedra, and lead to conforming triangulations. Second, we develop H^1 interpolation error estimates for the finite element space associated with the proposed anisotropic mesh. Due to the lack of regularity in the usual Sobolev space, these estimates are established for solutions in suitable weighted Sobolev spaces $\mathcal{M}^m_{\boldsymbol{\mu}}$ (Definition 2.2), in which the norm of the solution continuously depends on the given data f. Using the interpolation error estimates and weighted regularity results for the solution, one can decide the range of the grading parameters, such that the finite element solution approximates the singular solution in the optimal rate.

A notable difference from the existing meshes is that our triangulation, with tetrahedral elements, in general, violates the maximum angle condition [7]. Namely, the maximum interior angle in the triangular faces of the tetrahedra approaches π as the level of refinements increases. To overcome the resulting difficulty in the error analysis, we develop technical tools through the following steps. First, we classify tetrahedra into different types according to their relation with the singular set. For each tetrahedron type, we construct explicit linear transformations that map the tetrahedra to the reference element. We show that the mapping is bounded, whose upper bound is independent of the refinement level. Then, we obtain the interpolation error estimate by proving that the lack of angle condition can be compensated for by different weights in the function space. The finite element error estimate (Theorem 4.25) is an immediate consequence of the interpolation error analysis and the Céa Lemma. The weighted space $\mathcal{M}^m_{\boldsymbol{\mu}}$ and some of its variants are closely related to the Mellin transform for non-smooth domains [29, 30], in which

many rigorous regularity results have been established [16, 22, 24]. Thus, using $\mathcal{M}_{\boldsymbol{\mu}}^m$ as the function space for the solution, to validate the proposed FEM, here we pay more attention to the connection between the grading parameters in the anisotropic mesh and the indices in the weighted space. Besides the results in this paper, we also expect that the self-contained analytical techniques developed here will lead to new convergence results when similar weighted spaces are considered, and will be useful for other numerical studies of the proposed anisotropic FEM. In particular, we mention that $\mathcal{M}_{\boldsymbol{\mu}}^m$ is the space for the homogeneous Dirichlet problem (1). For problems with the Neumann or other boundary conditions, different weighted spaces that contain polynomials near the boundary may be needed to characterize the solution. We shall study the proposed anisotropic method in such weighted spaces for more general applications in future works.

The rest of the paper is organized as follows. In Section 2, we define the weighted Sobolev space and the finite element approximation to equation (1). In Section 3, we propose the 3D anisotropic mesh algorithm and discuss the resulting mesh properties. In Section 4, we give detailed interpolation error estimates on anisotropic meshes in weighted spaces. In Section 5, we report numerical test results on two model domains. These numerical results are in agreement with our theoretical prediction, and hence provide evidence for the validation of our method.

Throughout the text below, we adopt the bold notation for vector fields. Let T be a triangle (resp. tetrahedron) with vertices a, b, c (resp. a, b, c, d). Then, we denote T by its vertices: $\triangle^3 abc$ for the triangle and $\triangle^4 abcd$ for the tetrahedron, where the sup-index implies the number of vertices for T. We denote by ab the open line segment with endpoints a and b and denote by $\overrightarrow{ab}$ the vector from a to b. By $a \sim b$ (resp. $a \lesssim b$), we mean there exists a constant $C > 0$ independent of a and b, such that $C^{-1} a \leq b \leq Ca$ (resp. $a \leq Cb$). In addition, when $A \subset B$, it is possible that $A = B$. The generic constant $C > 0$ in our estimates may be different at different occurrences. It will depend on the computational domain, but not on the functions involved or the mesh level in the finite element algorithms.

2. Preliminaries

In this section, we introduce the weighted Sobolev space and the finite element approximation to equation (1), as well as other necessary notation and existing results.

2.1. **Weighted Sobolev spaces.** Let $\mathcal{V} = \{v_\ell\}_{\ell=1}^{N_v}$ and $\mathcal{E} = \{e_\ell\}_{\ell=1}^{N_e}$ be the set of vertices and *open* edges of Ω, where N_v and N_e are the numbers of the vertices and edges, respectively. Let $N_s := N_v + N_e$. Then, we denote the singular set by $\mathcal{S} := \{s_\ell\}_{\ell=1}^{N_s} = \mathcal{V} \cup \mathcal{E}$. We number the elements in $\mathcal{S}$, such that

(3) $s_\ell = v_\ell$ for $1 \leq \ell \leq N_v$; $s_\ell = e_{\ell-N_v}$ for $N_v < \ell \leq N_s$.

Namely, the first N_s elements are vertices, while the last N_e elements are edges.

Then, we classify different sub-regions based on their locations relative to the singular set $\mathcal{S}$.

Definition 2.1 (The domain decomposition)**.** For a vertex $v \in \mathcal{V}$, let $\mathcal{O}_v \subset \Omega$ be a neighborhood of v, whose closure does not contain any other vertices. Let $\mathcal{G}_v$ be the projection of $\mathcal{O}_v$ on the unit sphere S^2 centered at v. Therefore, $\mathcal{G}_v$ is a spherical polygon on S^2. Denote by $\mathcal{E}_v \subset \mathcal{E}$ the set of edges that touch v. Then,

each edge $e \in \mathcal{E}_v$ corresponds to a vertex v_e of the region $\mathcal{G}_v$. Let $\mathcal{O}(v_e) \subset \mathcal{G}_v$ be a neighborhood of the vertex v_e, whose closure does not contain other vertices of $\mathcal{G}_v$. Then, using the spherical coordinates $(\rho, \vartheta) \in \mathbb{R}_+ \times S^2$ centered at v, we define the neighborhood of the part of the edge $e \in \mathcal{E}_v$ close to v, $\mathcal{O}_e^v = \{(\rho, \vartheta) \in \mathcal{O}_v, \ \vartheta \in \mathcal{O}(v_e)\}$. Thus, Ω has the decomposition

$$(4) \qquad \Omega = \left(\bigcup_{v \in \mathcal{V}} \left(\mathcal{O}_v^o \cup \left(\bigcup_{e \in \mathcal{E}_v} \mathcal{O}_e^v \right) \right) \right) \cup \Omega^o \cup \left(\bigcup_{e \in \mathcal{E}} \mathcal{O}_e^o \right),$$

where $\mathcal{O}_v^o = \mathcal{O}_v \setminus (\bigcup_{e \in \mathcal{E}_v} \mathcal{O}_e^v)$, Ω^o is an interior region of Ω away from the singular points, and $\mathcal{O}_e^o = \Omega \setminus (\Omega^o \cup (\bigcup_{v \in \mathcal{V}} \mathcal{O}_v))$. Namely, Ω is decomposed into four components: (I) $\bigcup_{v \in \mathcal{V}}(\bigcup_{e \in \mathcal{E}_v} \mathcal{O}_e^v)$, the neighborhood of the part of edges close to vertices; (II) $\bigcup_{e \in \mathcal{E}} \mathcal{O}_e^o$, the neighborhood of the part of the edges away from vertices; (III) $\bigcup_{v \in \mathcal{V}} \mathcal{O}_v^o$, the sub-region of the neighborhood of the vertices that does not contain edge points; (IV) Ω^o, the interior part away from the singular set $\mathcal{S}$.

With this domain decomposition, we define the following weighted Sobolev space.

Definition 2.2 (Anisotropic weighted spaces). Let H^m, $m \geq 0$, be the usual Sobolev space that consists of functions whose kth derivatives are square-integrable for $0 \leq k \leq m$. Let $H_{loc}^m(\Omega) := \{v, \ v \in H^m(\omega)\}$, where ω is any open subset with compact closure $\bar{\omega} \subset \Omega$. Let $\rho_v(x)$ and $\rho_e(x)$ be distance functions from $x \in \Omega$ to the vertex $v \in \mathcal{V}$ and to the edge $e \in \mathcal{E}$, respectively. Within the neighborhood $\mathcal{O}_e^v$, let $\rho_{e,v} = \rho_e/\rho_v$ be the angular distance. In the neighborhoods $\mathcal{O}_e^o$ and $\mathcal{O}_e^v$, we choose a local Cartesian coordinate system in which the edge $e \in \mathcal{E}$ lies on the z-axis. Let $\alpha_\perp = (\alpha_1, \alpha_2)$ consist of the first two entries of the multi-index $\alpha = (\alpha_1, \alpha_2, \alpha_3) \in \mathbb{Z}_{\geq 0}^3$. Therefore, in $\mathcal{O}_e^o$ and $\mathcal{O}_e^v$, $\partial^{\alpha_\perp} = \partial_x^{\alpha_1} \partial_y^{\alpha_2}$ is a partial derivative in a direction perpendicular to the z-axis. Recall the singular set $\mathcal{S}$ in (3). Then, given an N_s-dimensional vector $\boldsymbol{\mu} = (\mu_1, \ldots, \mu_{N_s})$, we define the anisotropic weighted space

$$(5) \qquad \mathcal{M}_{\boldsymbol{\mu}}^m(\Omega) := \{v \in H_{loc}^m(\Omega), \ \rho_v^{|\alpha|-\mu_v} \partial^\alpha v \in L^2(\mathcal{O}_v^o), \ \rho_e^{|\alpha_\perp|-\mu_e} \partial^\alpha v \in L^2(\mathcal{O}_e^o),$$
$$\rho_v^{|\alpha|-\mu_v} \rho_{e,v}^{|\alpha_\perp|-\mu_e} \partial^\alpha v \in L^2(\mathcal{O}_e^v) \ \ \forall |\alpha| \leq m\},$$

where μ_v and μ_e are the entries in $\boldsymbol{\mu}$ that have the same sub-indices as those of v and e in $\mathcal{S}$. Thus, for $1 \leq \ell \leq N_v$, μ_ℓ specifies the weight associated to the vertex $v_\ell \in \mathcal{V}$; and for $N_v < \ell \leq N_s$, μ_ℓ gives the weight associated to the edges $e_{\ell-N_v} \in \mathcal{E}$. For any $v \in \mathcal{M}_{\boldsymbol{\mu}}^m(\Omega)$, the associated norm is

$$\|v\|_{\mathcal{M}_{\boldsymbol{\mu}}^m(\Omega)}^2 := \|v\|_{H^m(\Omega^o)}^2 + \sum_{|\alpha| \leq m} \Big(\sum_{v \in \mathcal{V}} [\|\rho_v^{|\alpha|-\mu_v} \partial^\alpha v\|_{L^2(\mathcal{O}_v^o)}^2$$

$$+ \sum_{\{e \in \mathcal{E}, \bar{e} \cap v = v\}} \|\rho_v^{|\alpha|-\mu_v} \rho_{e,v}^{|\alpha_\perp|-\mu_e} \partial^\alpha v\|_{L^2(\mathcal{O}_e^v)}^2] + \sum_{e \in \mathcal{E}} \|\rho_e^{|\alpha_\perp|-\mu_e} \partial^\alpha v\|_{L^2(\mathcal{O}_e^o)}^2 \Big).$$

In this paper, all the vectors denoted by the bold font have N_s entries. For any two vectors $\boldsymbol{a}$ and $\boldsymbol{b}$, we write $\boldsymbol{a} < (\leq, >, \geq) \ \boldsymbol{b}$ if each entry $a_\ell < (\leq, >, \geq) \ b_\ell$, $1 \leq \ell \leq N_s$. We denote by $\mathbf{1}$ (resp. $\mathbf{0}$) the constant N_s-dimensional vectors with all entries being 1 (resp. 0).

Note that the distance functions in the space $\mathcal{M}_{\boldsymbol{\mu}}^m$ are determined by the location of the singular set $\mathcal{S}$. Thus, they only depend on the domain Ω, and remain the same for any sub-region of Ω.

Remark 2.3. The space $\mathcal{M}_{\boldsymbol{\mu}}^m$ is anisotropic in the sense that the transverse derivatives $\partial^{\alpha_\perp}$ and the longitudinal derivatives along the edge play different roles in the formulation. Compared with the isotropic weighted spaces [16]

$$\mathcal{K}_{\boldsymbol{\mu}}^m(\Omega) := \{v \in H_{loc}^m(\Omega),\ \rho_v^{|\alpha|-\mu_v}\partial^\alpha v \in L^2(\mathcal{O}_v^o),\ \rho_e^{|\alpha|-\mu_e}\partial^\alpha v \in L^2(\mathcal{O}_e^o),$$
$$\rho_v^{|\alpha|-\mu_v}\rho_{e,v}^{|\alpha|-\mu_e}\partial^\alpha v \in L^2(\mathcal{O}_e^v)\ \forall |\alpha| \le m\},$$

the space $\mathcal{M}_{\boldsymbol{\mu}}^m$ is suitable to describe the anisotropic behavior of singular solutions, especially the additional regularity in the edge direction. For example, define the vector $\boldsymbol{\eta}$, such that

(6) $\eta_\ell = \sqrt{\lambda_\ell + 1/4}$ for $1 \le \ell \le N_v$ and $\eta_\ell = \pi/\omega_\ell$ for $N_v < \ell \le N_s$,

where $\lambda_\ell > 0$ is the smallest positive eigenvalue of the Laplace-Beltrami operator with the zero Dirichlet boundary condition on the spherical polygon $\mathcal{G}_{v_\ell}$ in the unit sphere S^2 centered at v_ℓ, and ω_ℓ is the interior dihedral angle of the edge $e_{\ell-N_v} \in \mathcal{E}$. Then, for $m \ge 0$, the solution $u \in H_0^1(\Omega)$ of equation (1), satisfies [16, 19]

(7) $$\|u\|_{\mathcal{M}_{\boldsymbol{a+1}}^m(\Omega)} \le C\|f\|_{\mathcal{M}_{\boldsymbol{a-1}}^m(\Omega)} \qquad \text{for } \boldsymbol{0} \le \boldsymbol{a} < \boldsymbol{\eta}.$$

This shows the continuous dependence of the solution on the given data in weighted spaces, despite the lack of regularity in usual Sobolev spaces.

Remark 2.4. Note that the estimate (7) does not give a shifting in the index m. In fact, a smoother f is expected in order for u to be in $\mathcal{M}_{\boldsymbol{a+1}}^{m+2}(\Omega)$ [11]. This, however, requires sophisticated regularity analysis that we will address in a forthcoming paper. Nevertheless, our goal in this paper is to propose new anisotropic finite element algorithms and develop interpolation error estimates in suitable weighted spaces. These estimates will also facilitate the finite element analysis for singular solutions when other anisotropic regularity results become available. Hence, from now on, we assume the solution of equation (1) satisfies

$$u \in \mathcal{M}_{\boldsymbol{\sigma+1}}^{m+1}(\Omega) \qquad \text{for } m \ge 1,$$

where $\boldsymbol{\sigma} > \boldsymbol{0}$ will be specified later.

2.2. **The finite element method.** Recall that $H_0^1(\Omega) \subset H^1(\Omega)$ is the subspace consisting of functions with zero trace on $\partial\Omega$. The variational solution $u \in H_0^1(\Omega)$ of equation (1) satisfies

$$a(u,v) = \int_\Omega \nabla u \cdot \nabla v dx = \int_\Omega f v dx = (f, v) \quad \forall v \in H_0^1(\Omega).$$

Let $\mathcal{T}_n$ be a triangulation of Ω with tetrahedra. Let $S_n \subset H_0^1(\Omega)$ be the Lagrange finite element space of degree $m \ge 1$ associated with $\mathcal{T}_n$. Namely, $S_n = \{v \in C(\Omega),\ v|_T \in \mathbb{P}_m,\ \text{for any tetrahedron } T \in \mathcal{T}_n\}$, where $\mathbb{P}_m$ is the space of polynomials of degree $\le m$. Then, the finite element solution $u_n \in S_n$ for equation (1) is defined by

(8) $$a(u_n, v_n) = (f, v_n) \quad \forall v_n \in S_n.$$

Remark 2.5. By the Poincaré inequality, the bilinear form $a(\cdot, \cdot)$ is both continuous and coercive on $H_0^1(\Omega)$. Thus, the Céa Lemma [14, 17] gives rise to

$$\text{(9)} \qquad \|u - u_n\|_{H^1(\Omega)} \leq \inf_{v_n \in S_n} \|u - v_n\|_{H^1(\Omega)}.$$

On a standard quasi-uniform triangulation $\mathcal{T}_n$, it is well known that the limited regularity of u in the usual Sobolev space may result in a *sub-optimal* convergence rate for the finite element approximation. Namely,

$$\text{(10)} \qquad \|u - u_n\|_{H^1(\Omega)} \leq Ch^s \|u\|_{H^{s+1}(\Omega)},$$

where h is the mesh size in $\mathcal{T}_n$ and $0 < s < m$ depends on the geometry of the domain.

3. ANISOTROPIC MESH ALGORITHMS

In this section, we propose new 3D anisotropic mesh algorithms for the finite element approximation of singular solutions of equation (1). We first classify tetrahedra in the triangulation based on their relation with the singular set $\mathcal{S}$.

Definition 3.1 (Tetrahedron types). Recall the vertex set $\mathcal{V}$, the edge set $\mathcal{E}$, and $\mathcal{S} = \mathcal{V} \cup \mathcal{E}$. For a tetrahedron T, we say T contains a *singular edge* if one of its edges lies on an edge in $\mathcal{E}$. Let x be a vertex of T. We say x is a *singular vertex* of T if $x \in \mathcal{V}$, or $x \in e$ for some edge $e \in \mathcal{E}$ but none of T's edges lies on e. Let $\mathcal{T}$ be an initial triangulation of Ω, such that: (I) each tetrahedron contains at most one singular vertex and at most one singular edge; (II) if a tetrahedron contains both a singular vertex and a singular edge, the singular vertex is an endpoint of the singular edge. Then, each tetrahedron $T \in \mathcal{T}$ falls into one of the five categories.

(1) *o*-tetrahedron: $\bar{T} \cap \mathcal{S} = \emptyset$.
(2) *v*-tetrahedron: $\bar{T} \cap \mathcal{S}$ is a vertex in $\mathcal{V}$.
(3) v_e-tetrahedron: $\bar{T} \cap \mathcal{S}$ is an interior point of an edge in $\mathcal{E}$.
(4) *e*-tetrahedron: $\bar{T} \cap \mathcal{S}$ is an edge of T, which lies on an edge in $\mathcal{E}$ but contains no vertex in $\mathcal{V}$.
(5) *ev*-tetrahedron: $\bar{T} \cap \mathcal{S}$ contains a vertex $v \in \mathcal{V}$ and an edge of T that lies on an edge in $\mathcal{E}$ joining v.

Then, we present our anisotropic mesh algorithm.

Algorithm 3.2 (Anisotropic refinement). *Let $\mathcal{T}$ be a triangulation of Ω as in Definition 3.1. For each element $s_\ell \in \mathcal{S}$, $1 \leq \ell \leq N_s$, we associate a grading parameter $\kappa_\ell \in (0, 1/2]$. Let $T = \triangle^4 x_0 x_1 x_2 x_3 \in \mathcal{T}$ be a tetrahedron with vertices x_0, x_1, x_2, x_3, such that x_0 is the singular vertex if T is a v-, v_e-, or ev-tetrahedron; and $x_0 x_1$ is the singular edge if T is an e- or ev-tetrahedron. Let $\boldsymbol{\kappa} = (\kappa_1, \ldots, \kappa_{N_s})$ be the collection of the grading parameters, such that each κ_ℓ corresponds to an element s_ℓ in the singular set $\mathcal{S}$. Then, the refinement, denoted by $\boldsymbol{\kappa}(\mathcal{T})$, proceeds as follows. We first generate new nodes x_{kl}, $0 \leq k < l \leq 3$, on each edge $x_k x_l$ of T, based on its type.*

(I) *(T is an o-tetrahedron):* $x_{kl} = (x_k + x_l)/2$.
(II) *(T is a v-tetrahedron): Suppose $x_0 = s_\ell \in \mathcal{V}$ ($1 \leq \ell \leq N_v$). Define $\kappa_v := \kappa_\ell$. Let $I_v := \{\ell, \ v \text{ is an endpoint of } e_{\ell - N_v}\}$ be the index set for edges touching v. Define $\kappa = \kappa_{ev} := \min_{\ell \in I_v}(\kappa_v, \kappa_\ell)$. Then, $x_{kl} = (x_k + x_l)/2$ for $1 \leq k < l \leq 3$; $x_{0l} = (1 - \kappa)x_0 + \kappa x_l$ for $1 \leq l \leq 3$.*
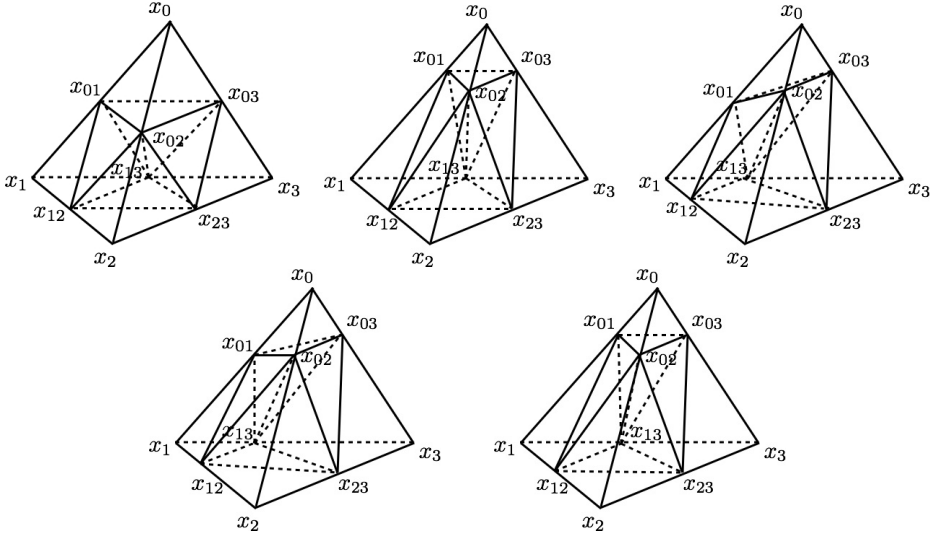
FIGURE 1. Decompositions for a tetrahedron $\triangle^4 x_0 x_1 x_2 x_3$, top row (left to right): o-tetrahedron, v- or v_e-tetrahedron, e-tetrahedron; bottom row (left to right): an ev-tetrahedron ($\kappa_v > \kappa_e$), an ev-tetrahedron ($\kappa_v < \kappa_e$).

(III) (T *is a v_e-tetrahedron*): *Suppose* $x_0 = \overline{x_0 x_1} \cap s_\ell$, $(N_v < \ell \leq N_s)$, *namely,* $s_\ell \in \mathcal{E}$. *We define* $\kappa = \kappa_e := \kappa_\ell$. *Then,* $x_{kl} = (x_k + x_l)/2$ *for* $1 \leq k < l \leq 3$; $x_{0l} = (1 - \kappa)x_0 + \kappa x_l$ *for* $1 \leq l \leq 3$.

(IV) (T *is an e-tetrahedron*): *Suppose* $x_0 x_1 \subset e_{\ell - N_v} = s_\ell \in \mathcal{E}$ $(N_v < \ell \leq N_s)$. *Define* $\kappa_e := \kappa_\ell$. *Then,* $x_{kl} = (1 - \kappa_e)x_k + \kappa_e x_l$ *for* $0 \leq k \leq 1$ *and* $2 \leq l \leq 3$; $x_{01} = (x_0 + x_1)/2$, $x_{23} = (x_2 + x_3)/2$.

(V) (T *is an ev-tetrahedron*): *Suppose* $x_0 = v_\ell = s_\ell \in \mathcal{V}$ $(1 \leq \ell \leq N_v)$ *and* $x_0 x_1 \subset e_{\ell' - N_v} = s_{\ell'} \in \mathcal{E}$ $(N_v < \ell' \leq N_s)$. *Define* $\kappa_v := \kappa_\ell$, $\kappa_e := \kappa_{\ell'}$, *and* $\kappa_{ev} := \min_{\ell \in I_v}(\kappa_v, \kappa_\ell)$, *where* I_v *is the index set defined in* (II). *Then, for* $2 \leq l \leq 3$, $x_{0l} = (1 - \kappa_{ev})x_0 + \kappa_{ev} x_l$ *and* $x_{1l} = (1 - \kappa_e)x_1 + \kappa_e x_l$; $x_{01} = (1 - \kappa_v)x_0 + \kappa_v x_1$, $x_{23} = (x_2 + x_3)/2$.

Connecting these nodes x_{kl} on all the faces of T, we obtain four sub-tetrahedra and one octahedron. The octahedron then is cut into four tetrahedra using x_{13} as the common vertex. Therefore, after one refinement, we obtain eight sub-tetrahedra for each $T \in \mathcal{T}$ denoted by their vertices:

$$\triangle^4 x_0 x_{01} x_{02} x_{03}, \ \triangle^4 x_1 x_{01} x_{12} x_{13}, \ \triangle^4 x_2 x_{02} x_{12} x_{23}, \ \triangle^4 x_3 x_{03} x_{13} x_{23},$$
$$\triangle^4 x_{01} x_{02} x_{03} x_{13}, \ \triangle^4 x_{01} x_{02} x_{12} x_{13}, \ \triangle^4 x_{02} x_{03} x_{13} x_{23}, \ \triangle^4 x_{02} x_{12} x_{13} x_{23}.$$

See Figure 1 for different types of decompositions. Given an initial mesh $\mathcal{T}_0$ satisfying the condition in Definition 3.1, the associated family of anisotropic meshes $\{\mathcal{T}_n, \ n \geq 0\}$ is defined recursively $\mathcal{T}_n = \boldsymbol{\kappa}(\mathcal{T}_{n-1})$. See Figure 2 for example.

Remark 3.3. Algorithm 3.2 first assigns to each singular element $s_\ell \in \mathcal{S}$ a grading parameter κ_ℓ, which can be regarded as an indicator of the severity of the singularity at s_ℓ. A smaller value of κ_ℓ leads to a higher mesh density near s_ℓ, while the value $\kappa_\ell = 1/2$ corresponds to a quasi-uniform refinement. It is apparent that our meshing
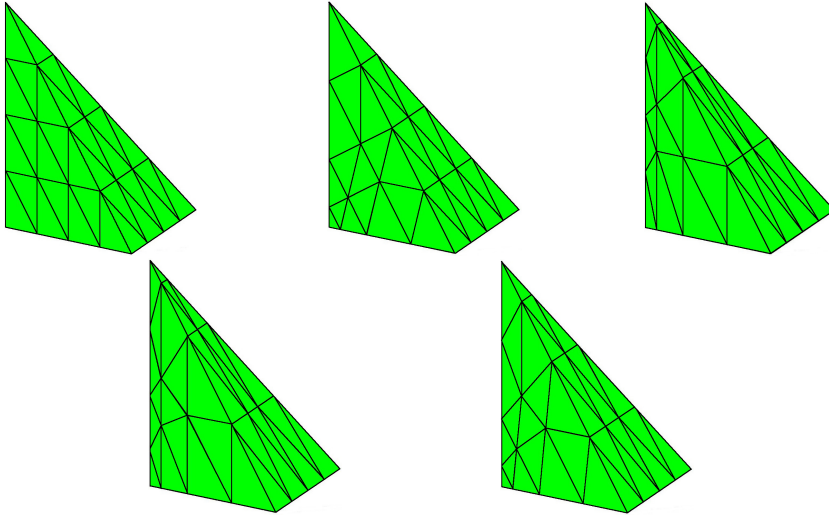
FIGURE 2. Anisotropic triangulations after two consecutive refinements on a tetrahedron, top row (left to right): o-tetrahedron, v- or v_e-tetrahedron ($\kappa = 0.3$), e-tetrahedron ($\kappa_e = 0.3$); bottom row (left to right): ev-tetrahedron ($\kappa_{ev} = 0.3, \kappa_v = 0.4, \kappa_e = 0.3$), ev-tetrahedron ($\kappa_{ev} = 0.3, \kappa_v = 0.3, \kappa_e = 0.4$).

method results in very different mesh geometries. In a region away from the singular set $\mathcal{S}$ (i.e., Ω^o), the mesh is isotropic and quasi-uniform. The local refinement for a v- or v_e-tetrahedron in fact follows the same rule: the mesh is isotropic and graded toward the vertex x_0 based on the grading parameter κ associated to the vertex x_0. In the neighborhood $\mathcal{O}_e^o$ of an edge away from the vertices, the resulting mesh in general is anisotropic and graded toward the edge $e \in \mathcal{E}$. The mesh refinement in $\mathcal{O}_e^v$ depends on the parameters κ_v and κ_ℓ, $\ell \in I_v$, which is also anisotropic, graded toward both the edge $e \in \mathcal{E}$ and the vertex $v \in \mathcal{V}$.

Remark 3.4. Our anisotropic refinements also generate tetrahedra with different shape regularities. A direct calculation shows that successive refinements of an o-tetrahedron produce tetrahedra within three similarity classes [13]; refinements for a v- or v_e-tetrahedron produce tetrahedra within 22 similarity classes (Remark 3.4 in [28]). However, refinements for an e- or ev-tetrahedron lead to anisotropic meshes toward the edge that in general do not preserve the maximum angle condition. Namely, the maximum edge angle in the face of the tetrahedron approaches π as the level of refinement n increases. This is a main difficulty that we shall overcome in the error analysis.

Remark 3.5. Compared with existing 3D graded mesh refinements [1, 3, 11, 38], the proposed algorithm has a few notable properties: (1) it is simple, explicit, and defined recursively; (2) the meshes $\mathcal{T}_j$, $j \leq n$, are conforming and the associated finite element spaces S_j are nested; (3) the algorithm results in a triangulation with the same topology and data structure as the usual 3D uniform mesh [13], and also provides the flexibility to adjust the grading parameters for vertex and edge singularities on general polyhedral domains. In what follows, we shall obtain

interpolation error estimates for singular solutions on such meshes, which in turn imply that our mesh can effectively improve the convergence of the finite element approximation.

To simplify the exposition in the next section, for a singular element in $\mathcal{S}$, we now define another set of parameters associated with κ_v, κ_e, and κ_{ev} (Algorithm 3.2). When $s_\ell \in \mathcal{S}$ is a vertex v, let a_v be such that

$$(11) \qquad \kappa_v = \kappa_\ell = 2^{-m/a_v}.$$

When $s_\ell \in \mathcal{S}$ is an edge e, let a_e be such that

$$(12) \qquad \kappa_e = \kappa_\ell = 2^{-m/a_e}.$$

In addition, we define the constant $a_{ev} = \min_{\ell \in I_v}(a_v, a_\ell)$, where I_v is the index set defined in (II) of Algorithm 3.2. Therefore,

$$(13) \qquad \kappa_{ev} = 2^{-m/a_{ev}}.$$

Then, we denote by $\boldsymbol{a} = (a_1, \dots, a_{N_s})$ the collection of these mesh parameters

$$(14) \qquad a_\ell := \begin{cases} a_{ev}, & \text{if } v = s_\ell; \\ a_e, & \text{if } e = s_\ell, \end{cases} \qquad 1 \leq \ell \leq N_s.$$

Here, $m \geq 1$ is the polynomial degree in the finite element approximation (8). Since $\kappa_\ell \in (0, 1/2]$, it is clear that $0 < a_\ell \leq m$.

4. Interpolation error estimates

In this section, we develop analytical tools and obtain interpolation error estimates on the proposed anisotropic mesh. Let $\mathcal{T}_0$ be an initial triangulation of the domain Ω with tetrahedra that satisfy the condition in Definition 3.1. Recall $\mathcal{T}_n$ is the mesh obtained after n successive refinements based on the parameter $\boldsymbol{\kappa}$. Throughout this section, we let $h := 2^{-n}$ be the mesh parameter of $\mathcal{T}_n$. For a continuous function v, we let v_I be its Lagrange nodal interpolation associated to the underlying mesh.

Note that the tetrahedra in the initial mesh $\mathcal{T}_0 = \{T_{(0),j}\}_{j=1}^J$ are all shape regular and can be classified into five categories (Definition 3.1). Thus, with the triangulation $\mathcal{T}_n$, the interpolation error estimates on Ω break down into the interpolation error estimates on the sub-regions of Ω, each of which is represented by an initial tetrahedron $T_{(0),j} \in \mathcal{T}_0$.

In addition, we mention that based on the definition, the space $\mathcal{M}_{\boldsymbol{\mu}}^{m+1}$, $m \geq 1$, regardless of the sub-index $\boldsymbol{\mu}$, is equivalent to the Sobolev space H^{m+1} on any sub-region of Ω that is away from the singular set $\mathcal{S}$. Therefore, by the Sobolev embedding Theorem, $u \in \mathcal{M}_{\boldsymbol{\mu}}^{m+1}(\Omega)$ is continuous at each nodal point in the interior of the domain. On the boundary of the domain, we set $u_I = 0$ due to the boundary condition. This makes the interpolation u_I well defined.

4.1. Estimates on initial o-, v-, and v_e-tetrahedra in $\mathcal{T}_0$. We first have the estimate for an o-tetrahedron in the initial mesh.

Lemma 4.1. *Let $T_{(0)} \in \mathcal{T}_0$ be an o-tetrahedron. For $u \in \mathcal{M}_{\boldsymbol{a+1}}^{m+1}(\Omega)$, where $\boldsymbol{a}$ is given in (14), let u_I be its nodal interpolation on $\mathcal{T}_n$. Then, we have*

$$(15) \qquad |u - u_I|_{H^1(T_{(0)})} \leq Ch^m \|u\|_{\mathcal{M}_{\boldsymbol{a+1}}^{m+1}(T_{(0)})},$$

where $h = 2^{-n}$ and C is independent of n and u.

Proof. Based on Algorithm 3.2, the restriction of $\mathcal{T}_n$ on $T_{(0)}$ is a quasi-uniform mesh with size $O(2^{-n})$. Since $H^{m+1}(T_{(0)})$ is equivalent to $\mathcal{M}_{a+1}^{m+1}(T_{(0)})$ on an o-tetrahedron, by the standard interpolation error estimate, we have

$$|u - u_I|_{H^1(T_{(0)})} \le C2^{-nm}\|u\|_{H^{m+1}(T_{(0)})} \le Ch^m\|u\|_{\mathcal{M}_{a+1}^{m+1}(T_{(0)})}.$$

This completes the proof. $\qquad\qquad\qquad\qquad\qquad\qquad\qquad\qquad\square$

For a v- or v_e-tetrahedron in $\mathcal{T}_0$, we first identify its sub-regions that have comparable distances to the singular vertex.

Definition 4.2 (Mesh layers in v- and v_e-tetrahedra). Let $T_{(0)} = \triangle^4 x_0 x_1 x_2 x_3 \in \mathcal{T}_0$ be either a v- or a v_e-tetrahedron with $x_0 \in \mathcal{V}$ or $x_0 \in e \in \mathcal{E}$. We use a local Cartesian coordinate system, such that x_0 is the origin. For $1 \le i \le n$, the ith refinement on $T_{(0)}$ produces a small tetrahedron with x_0 as a vertex and with one face, denoted by $P_{v,i}$, parallel to the face $\triangle^3 x_1 x_2 x_3$ of $T_{(0)}$. See Figure 1 for example.

Then, after n refinements, we define the ith mesh layer $L_{v,i}$ of $T_{(0)}$, $1 \le i < n$, as the region in $T_{(0)}$ between $P_{v,i}$ and $P_{v,i+1}$. We denote by $L_{v,0}$ the region in $T_{(0)}$ between $\triangle^3 x_1 x_2 x_3$ and $P_{v,1}$; and let $L_{v,n}$ be the small tetrahedron with x_0 as a vertex that is bounded by $P_{v,n}$ and three faces of $T_{(0)}$. Since it is clear that x_0 is the only point for the special refinement, we drop the sub-index ℓ in the grading parameter (14). Namely, for such $T_{(0)}$, we use

$$\kappa = 2^{-m/a}$$

to denote the grading parameter near x_0 ($\kappa = \kappa_{ev}$ if $x_0 \in \mathcal{V}$ and $\kappa = \kappa_e$ if $x_0 \in e \in \mathcal{E}$). Define the dilation matrix

$$(16) \qquad\qquad \mathbf{B}_{v,i} := \begin{pmatrix} \kappa^{-i} & 0 & 0 \\ 0 & \kappa^{-i} & 0 \\ 0 & 0 & \kappa^{-i} \end{pmatrix}.$$

Then, by Algorithm 3.2, $\mathbf{B}_{v,i}$ maps $L_{v,i}$ to $L_{v,0}$ for $0 \le i < n$, and maps $L_{v,n}$ to $T_{(0)}$. We define the *initial triangulation* of $L_{v,i}$, $0 \le i < n$, to be the first decomposition of $L_{v,i}$ into tetrahedra. Thus, the initial triangulation of $L_{v,i}$ consists of those tetrahedra in $\mathcal{T}_{i+1}$ that are contained in the layer $L_{v,i}$.

Remark 4.3. Based on the refinement, on $L_{v,i}$, $0 \le i \le n$, the tetrahedra in $\mathcal{T}_n$ are isotropic with mesh size $O(\kappa^i 2^{i-n})$. In $T_{(0)}$, let ρ be the distance to x_0. Therefore,

$$(17) \qquad\qquad\qquad \rho \sim \kappa^i \qquad \text{on } L_{v,i}, \quad 0 \le i < n.$$

Namely, if $T_{(0)}$ is a v-tetrahedron, $\rho \sim \rho_v$ for $v = x_0 \in \mathcal{V}$; and if $T_{(0)}$ is a v_e-tetrahedron, $\rho \sim \rho_e$, where $e \in \mathcal{E}$ is the edge containing x_0.

Then, we have the interpolation error estimate in the layer $L_{v,i}$.

Lemma 4.4. *Let $T_{(0)} \in \mathcal{T}_0$ be either a v- or a v_e-tetrahedron. For $u \in \mathcal{M}_{a+1}^{m+1}(\Omega)$, where $\boldsymbol{a}$ is given in (14), let u_I be its nodal interpolation on $\mathcal{T}_n$. Then, for $0 \le i < n$, we have*

$$|u - u_I|_{H^1(L_{v,i})} \le Ch^m\|u\|_{\mathcal{M}_{a+1}^{m+1}(L_{v,i})},$$

where $h = 2^{-n}$ and C is independent of n and u.

Proof. For $(x, y, z) \in L_{v,i}$, let $(\hat{x}, \hat{y}, \hat{z}) \in L_{v,0}$ be its image under the dilation $\mathbf{B}_{v,i}$. For a function v on $L_{v,i}$, we define $\hat{v}$ on $L_{v,0}$ by

$$\hat{v}(\hat{x}, \hat{y}, \hat{z}) := v(x, y, z).$$

As part of $\mathcal{T}_n$, the triangulation on $L_{v,i}$ is mapped by $\mathbf{B}_{v,i}$ to a triangulation on $L_{v,0}$ with mesh size $O(2^{i-n})$. Then, by the scaling argument and (17), we have

$$\begin{aligned} |u - u_I|^2_{H^1(L_{v,i})} = \kappa^i |\hat{u} - \hat{u}_I|^2_{H^1(L_{v,0})} &\leq C\kappa^i 2^{2m(i-n)} |\hat{u}|^2_{H^{m+1}(L_{v,0})} \\ &\leq C 2^{2m(i-n)} \kappa^{2mi} |u|^2_{H^{m+1}(L_{v,i})} \\ &\leq C 2^{2m(i-n)} \kappa^{2ai} \sum_{|\alpha|=m+1} \|\rho^{m-a} \partial^\alpha u\|^2_{L^2(L_{v,i})}. \end{aligned}$$

Recall $\kappa = 2^{-m/a}$ and Remark 4.3. Then, by the definition of the weighted space, we have

$$|u - u_I|^2_{H^1(L_{v,i})} \leq C 2^{2m(i-n)} \kappa^{2ai} \sum_{|\alpha|=m+1} \|\rho^{m-a} \partial^\alpha u\|^2_{L^2(L_{v,i})} \leq C h^{2m} \|u\|^2_{\mathcal{M}^{m+1}_{a+1}(L_{v,i})},$$

which completes the proof. □

Then, we give the error estimate on the entire initial tetrahedron $T_{(0)}$.

Corollary 4.5. *Let $T_{(0)} \in \mathcal{T}_0$ be either a v- or a v_e-tetrahedron. For $u \in \mathcal{M}^{m+1}_{a+1}(\Omega)$, where $\boldsymbol{a}$ is given in (14), let u_I be its nodal interpolation on $\mathcal{T}_n$. Then, we have*

$$|u - u_I|_{H^1(T_{(0)})} \leq C h^m \|u\|_{\mathcal{M}^{m+1}_{a+1}(T_{(0)})},$$

where $h = 2^{-n}$ and C is independent of n and u.

Proof. By Lemma 4.4, it suffices to show the estimate for the last layer $L_{v,n}$. For $(x, y, z) \in L_{v,n}$, let $(\hat{x}, \hat{y}, \hat{z}) \in T_{(0)}$ be its image under the dilation $\mathbf{B}_{v,n}$. For a function v on $L_{v,n}$, we define $\hat{v}$ on $T_{(0)}$ by

$$\hat{v}(\hat{x}, \hat{y}, \hat{z}) := v(x, y, z).$$

Now let χ be a smooth cutoff function on $T_{(0)}$ such that $\chi = 0$ in a neighborhood of x_0 and $= 1$ at every other node of $T_{(0)}$. Recall the distance function ρ from Remark 4.3. Thus, $\rho(\hat{x}, \hat{y}, \hat{z}) = \kappa^{-n} \rho(x, y, z)$. Since $\chi \hat{u} = 0$ in the neighborhood of x_0, we have

$$|\chi \hat{u}|^2_{H^{m+1}(T_{(0)})} \leq C \sum_{|\alpha| \leq m+1} \|\rho^{|\alpha|-1} \partial^\alpha \hat{u}\|^2_{L^2(T_{(0)})}.$$

Define $\hat{w} := \hat{u} - \chi \hat{u}$ and note that $(\chi \hat{u})_I = \hat{u}_I$. We have

$$\begin{aligned} (18) \qquad |\hat{u} - \hat{u}_I|_{H^1(T_{(0)})} = |\hat{w} + \chi \hat{u} - \hat{u}_I|_{H^1(T_{(0)})} &\leq |\hat{w}|_{H^1(T_{(0)})} + |\chi \hat{u} - \hat{u}_I|_{H^1(T_{(0)})} \\ &= |\hat{w}|_{H^1(T_{(0)})} + |\chi \hat{u} - (\chi \hat{u})_I|_{H^1(T_{(0)})} \\ &\leq C(\|\hat{u}\|_{H^1(T_{(0)})} + |\chi \hat{u}|_{H^{m+1}(T_{(0)})}), \end{aligned}$$

where C depends on m and, through χ, the nodes in the triangulation. Then, using (18), the scaling argument, $\kappa^{-n} \lesssim \rho^{-1}$ in $L_{v,n}$, the definition of the weighted space,

and (14), we have

$$|u - u_I|^2_{H^1(L_{v,n})} = \kappa^n |\hat{u} - \hat{u}_I|^2_{H^1(T_{(0)})}$$

$$\leq C\kappa^n (\|\hat{u}\|^2_{H^1(T_{(0)})} + \sum_{|\alpha| \leq m+1} \|\rho^{|\alpha|-1} \partial^\alpha \hat{u}\|^2_{L^2(T_{(0)})})$$

$$\leq C \sum_{|\alpha| \leq m+1} \|\rho^{|\alpha|-1} \partial^\alpha u\|^2_{L^2(L_{v,n})} \leq C\kappa^{2na} \|u\|^2_{\mathcal{M}^{m+1}_{a+1}(L_{v,n})}$$

$$= C2^{-2mn} \|u\|^2_{\mathcal{M}^{m+1}_{a+1}(L_{v,n})} = Ch^{2m} \|u\|^2_{\mathcal{M}^{m+1}_{a+1}(L_{v,n})}.$$

Then, the desired estimate follows by summing up the estimates from different layers $L_{v,i}$, $0 \leq i \leq n$. □

4.2. Estimates on initial e-tetrahedra in $\mathcal{T}_0$. Throughout this subsection, let $T_{(0)} := \triangle^4 x_0 x_1 x_2 x_3 \in \mathcal{T}_0$ be an e-tetrahedron with $x_0 x_1$ on the edge $e \in \mathcal{E}$ and let κ_e be the associated grading parameter. Then, we define the mesh layer associated with $\mathcal{T}_n$ on $T_{(0)}$ as follows.

Definition 4.6 (Mesh layers in e-tetrahedra). Based on Algorithm 3.2, in each refinement, an e-tetrahedron is cut by a parallelogram parallel to $x_0 x_1$. For example, in the e-tetrahedron of Figure 1, the quadrilateral with vertices $x_{02}, x_{12}, x_{13}, x_{03}$ is the aforementioned parallelogram. We denote by $P_{e,i}$ the parallelogram produced in the ith refinement, $1 \leq i \leq n$. Therefore, the distance from $P_{e,i+1}$ to e is $\kappa_e \times$ the distance from $P_{e,i}$ to e. For the mesh $\mathcal{T}_n$, let the ith layer $L_{e,i}$ on $T_{(0)}$, $0 < i < n$, be the region bounded by $P_{e,i}$, $P_{e,i+1}$, and the faces of $T_{(0)}$. Define $L_{e,0}$ to be the sub-region of $T_{(0)}$ away from e that is separated by $P_{e,1}$. We define $L_{e,n}$ to be the sub-region of $T_{(0)}$ between $P_{e,n}$ and e. See for example Figure 4. As in Definition 4.2, the initial triangulation of the layer $L_{e,i}$, $0 \leq i < n$, is the first decomposition of this region into tetrahedra. Thus, the initial triangulation of $L_{e,i}$ consists of those tetrahedra in $\mathcal{T}_{i+1}$ that are contained in $L_{e,i}$.

Remark 4.7. In the mesh layers, the distance ρ_e to the edge e satisfies

$$(19) \qquad\qquad \rho_e \sim \kappa_e^i \qquad \text{on } L_{e,i}, \quad 0 \leq i < n.$$

In addition, the mesh layers of an e-tetrahedron $T_{(0)}$ also satisfy the following properties (see Figure 4):

- The layer $L_{e,i}$, $2 \leq i \leq n$, is the union of two components: sub-regions from 2^{i-1} e-tetrahedra in $\mathcal{T}_{i-1}$ and sub-regions from $2^i - 2$ v_e-tetrahedra in $\mathcal{T}_{i-1}$.
- Among the aforementioned $2^i - 2$ v_e-tetrahedra in $\mathcal{T}_{i-1}$, 2^k of them are sub-regions of v_e-tetrahedra in $\mathcal{T}_k$, $1 \leq k \leq i - 1$.

Now, we start to develop some estimates for the shape regularity of the mesh on $L_{e,i}$, although it is in general anisotropic and violates the maximum angle condition. These results will be used for the interpolation error analysis.

Definition 4.8. (Relative distances for e-tetrahedra) Recall the initial e-tetrahedron $T_{(0)} = \triangle^4 x_0 x_1 x_2 x_3 \in \mathcal{T}_0$. For an e-tetrahedron $T = \triangle^4 \gamma_0 \gamma_1 \gamma_2 \gamma_3$ generated by some subsequent refinements of $T_{(0)}$ based on Algorithm 3.2, consider its two vertices on the edge $x_0 x_1$. We call the vertex that is closer to x_0 the *first vertex* of T, and call the vertex closer to x_1 the *second vertex* of T.

Without loss of generality, we suppose $\gamma_0 \gamma_1 \subset e \in \mathcal{E}$ and γ_0 (resp. γ_1) is the *first* (resp. *second*) vertex of T. Let γ be either γ_2 or γ_3. Denote by γ' the orthogonal

FIGURE 3. The mesh on an e-tetrahedron after one refinement (left); the induced triangles on a face containing the singular edge (right).

projection of γ on the z-axis (the axis containing the edge e). See for instance Figure 3. Then, we define $c_{\gamma,1}$ to be the *first relative z-distance* of γ, such that

$$(20) \qquad |c_{\gamma,1}| = |\gamma_0\gamma'|/|\gamma_0\gamma_1|, \quad \text{and}$$

$$\begin{cases} c_{\gamma,1} = |c_{\gamma,1}| & \text{if } \overrightarrow{\gamma_0\gamma'} = t(\overrightarrow{\gamma_0\gamma_1}) \text{ for some } t > 0, \\ c_{\gamma,1} = -|c_{\gamma,1}| & \text{otherwise.} \end{cases}$$

The *second relative z-distance* of γ, denoted by $c_{\gamma,2}$, is defined by

$$(21) \qquad |c_{\gamma,2}| = |\gamma_1\gamma'|/|\gamma_0\gamma_1|, \quad \text{and}$$

$$\begin{cases} c_{\gamma,2} = |c_{\gamma,2}| & \text{if } \overrightarrow{\gamma_1\gamma'} = t(\overrightarrow{\gamma_1\gamma_0}) \text{ for some } t > 0, \\ c_{\gamma,2} = -|c_{\gamma,2}| & \text{otherwise.} \end{cases}$$

It is clear that $c_{\gamma,2} = 1 - c_{\gamma,1}$. In addition, we define the *absolute relative distance* for T, denoted by c_T, such that

$$(22) \qquad c_T = \max(|c_{\gamma_2,1}|, \ |c_{\gamma_2,2}|, \ |c_{\gamma_3,1}|, \ |c_{\gamma_3,2}|).$$

Remark 4.9. For each e-tetrahedron, there are four relative distances corresponding to the two vertices away from the z-axis. The sign of the relative distance is determined by the location of orthogonal projection of the off-the-edge vertex. The relative distances imply, for the e-tetrahedron, how far the off-the-edge vertices shift away in the z-direction from the vertices on the z-axis.

Remark 4.10. Note that after one refinement, T is decomposed into eight sub-tetrahedra: two e-tetrahedra (denoted by T_A and T_B), two v_e-tetrahedra, and four o-tetrahedra. In this case, we call T the *parent tetrahedron* of the sub-tetrahedra, and call each sub-tetrahedron the *child tetrahedron* of T. Note that Definition 4.8 is also valid for ev-tetrahedra. We shall use it later for ev-tetrahedra as well.

In what follows, we establish the connections between T and its child e-tetrahedra T_A and T_B in terms of the corresponding relative z-distances.

Lemma 4.11. *Let $T \subset T_{(0)}$ be an e-tetrahedron in $\mathcal{T}_i$, $1 \leq i < n$. Let T_A, $T_B \subset T$ be the two child e-tetrahedra in $\mathcal{T}_{i+1}$. Denote by c_T, c_A, and c_B the absolute distances for T, T_A, and T_B as in (22). Then, $\max(c_A, c_B) \leq \max(c_T, 1)$.*

Proof. Denote T by $T = \triangle^4\gamma_0\gamma_1\gamma_2\gamma_3$ with the *first* vertex γ_0 and the *second* vertex γ_1 on the singular edge $\gamma_0\gamma_1$. As illustrated in Figure 3, we let $T_A := \triangle^4\gamma_0\gamma_4\gamma_5\gamma_6$

and $T_B := \triangle^4 \gamma_1 \gamma_4 \gamma_7 \gamma_8$. Recall the relative distance from Definition 4.8. In particular, let $c_{\gamma_2,1}, c_{\gamma_2,2}$ be the relative distances of γ_2 in T, and let $c_{\gamma_5,1}^A, c_{\gamma_5,2}^A$ (resp. $c_{\gamma_7,1}^B, c_{\gamma_7,2}^B$) be the relative distances of γ_5 (resp. γ_7) in T_A (resp. T_B). We first show $|c_{\gamma_5,1}^A|, |c_{\gamma_5,2}^A| \leq \max(|c_{\gamma_2,1}|, |c_{\gamma_2,2}|, 1)$.

Consider the triangles on the face $\triangle^3 \gamma_0 \gamma_1 \gamma_2$ of T, induced by the sub-tetrahedra after one refinement of T (the second picture in Figure 3). In addition, we have drawn three dashed line segments $\gamma_2 \gamma_2'$, $\gamma_5 \gamma_5'$, and $\gamma_7 \gamma_7'$ that are perpendicular to $\gamma_0 \gamma_1$. Then, by (20), we have

$$|c_{\gamma_2,1}| = |\gamma_0 \gamma_2'|/|\gamma_0 \gamma_1| \quad \text{and} \quad |c_{\gamma_5,1}^A| = |\gamma_0 \gamma_5'|/|\gamma_0 \gamma_4|.$$

Note that $\triangle^3 \gamma_0 \gamma_5 \gamma_5'$ is similar to $\triangle^3 \gamma_0 \gamma_2 \gamma_2'$. Therefore, $|\gamma_0 \gamma_5'| = \kappa_e |\gamma_0 \gamma_2'|$, and $c_{\gamma_2,1}$ and $c_{\gamma_5,1}^A$ have the same sign. Recall $0 < \kappa_e \leq 1/2$. Then, we consider all the possible cases.

In the case $c_{\gamma_2,1} < 0$, we have

$$0 > c_{\gamma_5,1}^A = -|\gamma_0 \gamma_5'|/|\gamma_0 \gamma_4| = -2\kappa_e |\gamma_0 \gamma_2'|/|\gamma_0 \gamma_1| = 2\kappa_e c_{\gamma_2,1} \geq c_{\gamma_2,1}.$$

Therefore, $|c_{\gamma_5,1}^A| \leq |c_{\gamma_2,1}|$. Meanwhile, we have

$$1 \leq c_{\gamma_5,2}^A = 1 - c_{\gamma_5,1}^A = 1 - 2\kappa_e c_{\gamma_2,1} < 1 - c_{\gamma_2,1} = c_{\gamma_2,2}.$$

Therefore, $|c_{\gamma_5,2}^A| \leq |c_{\gamma_2,2}|$.

In the case $0 \leq c_{\gamma_2,1} < (2\kappa_e)^{-1}$, we have $c_{\gamma_5,1}^A \geq 0$ and

$$c_{\gamma_5,1}^A = |\gamma_0 \gamma_5'|/|\gamma_0 \gamma_4| = 2\kappa_e |\gamma_0 \gamma_2'|/|\gamma_0 \gamma_1| = 2\kappa_e c_{\gamma_2,1} < 1.$$

Meanwhile, we have

$$0 \leq c_{\gamma_5,2}^A = 1 - c_{\gamma_5,1}^A = 1 - 2\kappa_e c_{\gamma_2,1} < 1.$$

In the case $c_{\gamma_2,1} \geq (2\kappa_e)^{-1}$, we have

$$1 \leq c_{\gamma_5,1}^A = |\gamma_0 \gamma_5'|/|\gamma_0 \gamma_4| = 2\kappa_e |\gamma_0 \gamma_2'|/|\gamma_0 \gamma_1| = 2\kappa_e c_{\gamma_2,1} \leq |c_{\gamma_2,1}|.$$

Meanwhile, we have

$$0 \geq c_{\gamma_5,2}^A = 1 - c_{\gamma_5,1}^A = 1 - 2\kappa_e c_{\gamma_2,1} \geq 1 - c_{\gamma_2,1} = c_{\gamma_2,2}.$$

Therefore, $|c_{\gamma_5,2}^A| \leq |c_{\gamma_2,2}|$. Thus, we have shown

$$|c_{\gamma_5,1}^A|, |c_{\gamma_5,2}^A| \leq \max(|c_{\gamma_2,1}|, |c_{\gamma_2,2}|, 1).$$

With a similar calculation, we can derive the upper bounds for other relative distances in T_A and T_B, namely,

$$|c_{\gamma_6,1}^A|, |c_{\gamma_6,2}^A| \leq \max(|c_{\gamma_3,1}|, |c_{\gamma_3,2}|, 1),$$

$$|c_{\gamma_7,1}^B|, |c_{\gamma_7,2}^B| \leq \max(|c_{\gamma_2,1}|, |c_{\gamma_2,2}|, 1), \quad |c_{\gamma_8,1}^B|, |c_{\gamma_8,2}^B| \leq \max(|c_{\gamma_3,1}|, |c_{\gamma_3,2}|, 1).$$

Hence, the proof is completed by (22). $\square$

Recall that for a v- or v_e-tetrahedron in $\mathcal{T}_0$, the isotropic transformation (16) maps a mesh layer to a reference domain (either the tetrahedron itself or the layer $L_{v,0}$). Here, we define the reference domain for an e-tetrahedron.
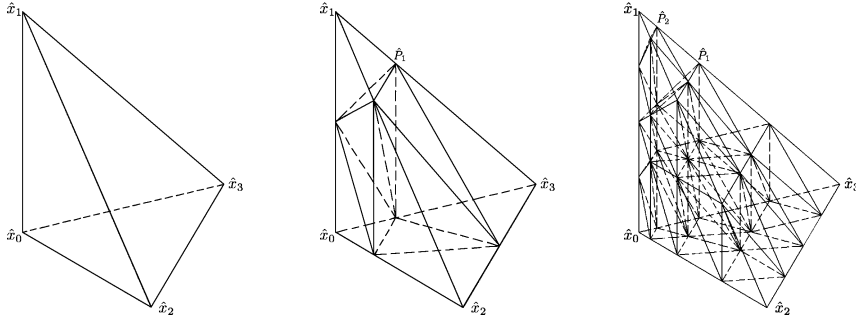
FIGURE 4. A reference tetrahedron $\hat{T}$ (left); the triangulation $\hat{\mathcal{T}}_1$ after one edge refinement (center); the triangulation $\hat{\mathcal{T}}_2$ after two edge refinements (right).

Definition 4.12 (The reference e-tetrahedron)**.** For the initial e-tetrahedron $T_{(0)} := \triangle^4 x_0 x_1 x_2 x_3 \in \mathcal{T}_0$, we use a local Cartesian coordinate system, such that the z-axis contains the edge $x_0 x_1$ with the direction of $\overrightarrow{x_0 x_1}$ as the positive direction, and x_2 is in the xz-plane. We will specify the origin later. Let $l_0 := |x_0 x_1|$ be the length of the singular edge. Then, we define the reference tetrahedron $\hat{T} = \triangle^4 \hat{x}_0 \hat{x}_1 \hat{x}_2 \hat{x}_3$, such that

$$\hat{x}_0 = (0, 0, -l_0/2), \quad \hat{x}_1 = (0, 0, l_0/2), \quad \hat{x}_k = (\hat{\lambda}_k, \hat{\xi}_k, -l_0/2), \ k = 2, 3,$$

where $\hat{\lambda}_k, \hat{\xi}_k$ are the x- and y-components of the vertices x_2 and x_3, respectively. Therefore, $\hat{\xi}_2 = 0$ and $\hat{\lambda}_2, \hat{\lambda}_3, \hat{\xi}_3$ are constants that depend on the shape regularity of $T_{(0)}$. Thus, $\hat{T}$ is a tetrahedron with one face in the plane $z = -l_0/2$, one face in the xz-plane, such that $|\hat{x}_0 \hat{x}_1| = |x_0 x_1|$, $|\hat{x}_0 \hat{x}_2| =$ the length of the orthogonal projection of $x_0 x_2$ in the plane $z = -l_0/2$, and $|\hat{x}_0 \hat{x}_3| =$ the length of the orthogonal projection of $x_0 x_3$ in the plane $z = -l_0/2$. In addition, we denote by $\hat{\mathcal{T}}_1$ and $\hat{\mathcal{T}}_2$ the triangulations of $\hat{T}$ after one and two edge refinements with parameter κ_e, respectively. See Figure 4 for example.

In the following lemmas, we construct explicit linear mappings between an e-tetrahedron $\subset T_{(0)}$ and the reference tetrahedron $\hat{T}$.

Lemma 4.13. *For an e-tetrahedron $\mathcal{T}_i \ni T := \triangle^4 \gamma_0 \gamma_1 \gamma_2 \gamma_3 \subset T_{(0)}$, $1 \leq i \leq n$, suppose $\gamma_0 \gamma_1$ is the singular edge, and $\overrightarrow{\gamma_0 \gamma_1}$ and $\overrightarrow{x_0 x_1}$ share the same direction. We use the local coordinate system in Definition 4.12, and set $(\gamma_0 + \gamma_1)/2$ to be the origin. Then, there exist a matrix*

$$(23) \qquad \mathbf{B}_{e,i} = \begin{pmatrix} \kappa_e^{-i} & 0 & 0 \\ 0 & \kappa_e^{-i} & 0 \\ b_1 \kappa_e^{-i} & b_2 \kappa_e^{-i} & 2^i \end{pmatrix}$$

with $|b_1|, |b_2| \leq C_0$, where $C_0 > 0$ depends on the initial tetrahedron $T_{(0)}$ but not on i, such that $\mathbf{B}_{e,i} : T \to \hat{T}$ is a bijection.

Proof. Based on the refinement in Algorithm 3.2, and on Definition 4.12, we have $\gamma_2 = (\kappa_e^i \hat{\lambda}_2, 0, \zeta_2)$, $\gamma_3 = (\kappa_e^i \hat{\lambda}_3, \kappa_e^i \hat{\xi}_3, \zeta_3)$, and $|\gamma_0 \gamma_1| = 2^{-i} l_0 = 2^{-i} |x_0 x_1|$, where ζ_2 and ζ_3 are the z-coordinates of the vertices γ_2 and γ_3, respectively. Thus, the

anisotropic transformation

$$\mathbf{A}_1 := \begin{pmatrix} \kappa_e^{-i} & 0 & 0 \\ 0 & \kappa_e^{-i} & 0 \\ 0 & 0 & 2^i \end{pmatrix}$$

maps T to a tetrahedron, with vertices $\mathbf{A}_1\gamma_0 = (0,0,-l_0/2)$, $\mathbf{A}_1\gamma_1 = (0,0,l_0/2)$, $\mathbf{A}_1\gamma_2 = (\hat{\lambda}_2, 0, 2^i\zeta_2)$, and $\mathbf{A}_1\gamma_3 = (\hat{\lambda}_3, \hat{\xi}_3, 2^i\zeta_3)$. Now, define

$$(24) \qquad b_1 = -(2^i\zeta_2 + 2^{-1}l_0)/\hat{\lambda}_2, \quad b_2 = [2^i(\zeta_2\hat{\lambda}_3 - \hat{\lambda}_2\zeta_3) + 2^{-1}l_0(\hat{\lambda}_3 - \hat{\lambda}_2)]/\hat{\lambda}_2\hat{\xi}_3,$$

and let

$$\mathbf{A}_2 := \begin{pmatrix} 1 & 0 & 0 \\ 0 & 1 & 0 \\ b_1 & b_2 & 1 \end{pmatrix}.$$

Then, a straightforward calculation shows that

$$\mathbf{B}_{e,i} := \mathbf{A}_2\mathbf{A}_1 = \begin{pmatrix} \kappa_e^{-i} & 0 & 0 \\ 0 & \kappa_e^{-i} & 0 \\ b_1\kappa_e^{-i} & b_2\kappa_e^{-i} & 2^i \end{pmatrix}$$

maps T to $\hat{T}$. Meanwhile, by Lemma 4.11, we have $|\zeta_2|, |\zeta_3| \leq C|\gamma_0\gamma_1| = C2^{-i}l_0$, where C depends on the shape regularity of $T_{(0)}$. In addition, since $\hat{\lambda}_2, \hat{\lambda}_3, \hat{\xi}_3$ all depend on the shape regularity of $T_{(0)}$ and $\hat{\lambda}_2, \hat{\xi}_3 \neq 0$, by (24), we conclude $|b_1|, |b_2| \leq C_0$, where $C_0 \geq 0$ depends on $T_{(0)}$ but not on i. $\square$

Recall the parent and child tetrahedra associated to each mesh refinement in Remark 4.10. Note that for a v_e-tetrahedron $T_{(i)} \subset T_{(0)}$ in $\mathcal{T}_i$, its parent tetrahedron, which is in $\mathcal{T}_{i-1}$, can be either a v_e-tetrahedron or an e-tetrahedron. Nevertheless, there exists a v_e-tetrahedron $T_{(k)} \in \mathcal{T}_k$, $1 \leq k \leq i$, such that $T_{(i)} \subset T_{(k)} \subset T_{(0)}$ and $T_{(k)}$'s parent tetrahedron is an e-tetrahedron in $\mathcal{T}_{k-1}$.

Next, we construct the mapping between a v_e-tetrahedron in $\mathcal{T}_i$ and the reference domain. Recall the triangulations $\hat{\mathcal{T}}_1$ and $\hat{\mathcal{T}}_2$ of $\hat{T}$ in Definition 4.12.

Lemma 4.14. *Let $T_{(i)} \subset T_{(0)}$ be a v_e-tetrahedron in $\mathcal{T}_i$, $1 \leq i \leq n$. Let $T_{(k)} \in \mathcal{T}_k$, $1 \leq k \leq i$, be the v_e-tetrahedron, such that $T_{(i)} \subset T_{(k)}$ and $T_{(k)}$'s parent tetrahedron $T_{(k-1)} = \triangle^4\gamma_0\gamma_1\gamma_2\gamma_3 \in \mathcal{T}_{k-1}$ is an e-tetrahedron. On $T_{(k-1)}$, we use the same local coordinate system as in Lemma 4.13 with origin at $(\gamma_0 + \gamma_1)/2$. Then, there is the transformation*

$$(25) \qquad \mathbf{B}_{i,k} = \begin{pmatrix} \kappa_e^{-i+1} & 0 & 0 \\ 0 & \kappa_e^{-i+1} & 0 \\ b_1\kappa_e^{-i+1} & b_2\kappa_e^{-i+1} & 2^{k-1}\kappa_e^{k-i} \end{pmatrix}$$

that maps $T_{(i)}$ to a v_e-tetrahedron in $\hat{\mathcal{T}}_1$, where $|b_1|, |b_2| \leq C_0$, for $C_0 > 0$ depending on $T_{(0)}$ but not on i or k.

Proof. Based on Algorithm 3.2, the origin $(\gamma_0 + \gamma_1)/2$ is the vertex of $T_{(i)}$ on the singular edge. Then, the linear mapping

$$\mathbf{A}_1 = \begin{pmatrix} \kappa_e^{k-i} & 0 & 0 \\ 0 & \kappa_e^{k-i} & 0 \\ 0 & 0 & \kappa_e^{k-i} \end{pmatrix}$$

translates $T_{(i)}$ to $T_{(k)}$. Since $T_{(k-1)}$ is an e-tetrahedron, by Lemma 4.13, the transformation

$$\mathbf{A}_2 = \begin{pmatrix} \kappa_e^{-k+1} & 0 & 0 \\ 0 & \kappa_e^{-k+1} & 0 \\ b_1\kappa_e^{-k+1} & b_2\kappa_e^{-k+1} & 2^{k-1} \end{pmatrix}$$

maps $T_{(k-1)}$ to $\hat{T}$, and also maps the restriction of $\mathcal{T}_k$ on $T_{(k-1)}$ to $\hat{\mathcal{T}}_1$, where $|b_1|, |b_2| < C$ for C depending on $T_{(0)}$. Therefore,

$$\mathbf{B}_{i,k} := \mathbf{A}_2\mathbf{A}_1 = \begin{pmatrix} \kappa_e^{-i+1} & 0 & 0 \\ 0 & \kappa_e^{-i+1} & 0 \\ b_1\kappa_e^{-i+1} & b_2\kappa_e^{-i+1} & 2^{k-1}\kappa_e^{k-i} \end{pmatrix}$$

maps $T_{(i)}$ to one of the v_e-tetrahedra in $\hat{\mathcal{T}}_1$. This completes the proof. $\qquad\square$

The parameters b_1 and b_2 in Lemmas 4.13 and 4.14 can be different for different tetrahedra in $\mathcal{T}_i$, but they are uniformly bounded by a constant that depends on the initial tetrahedron $T_{(0)}$. Now, we are ready to construct the mapping from a tetrahedron $T_{(i+1)} \in \mathcal{T}_{i+1}$ in the mesh layer $L_{e,i}$ (Definition 4.6) to the reference domain. Also recall that $T_{(i+1)}$ is a tetrahedron in the initial triangulation of $L_{e,i}$.

Lemma 4.15. *Let $T_{(i+1)} \in \mathcal{T}_{i+1}$ be a tetrahedron, such that $T_{(i+1)} \subset L_{e,i} \subset T_{(0)}$, $0 \le i < n$.*

Case 1. $T_{(i+1)}$ is a child tetrahedron of an e-tetrahedron $T_{(i)} \in \mathcal{T}_i$. Using the $T_{(i)}$-based local coordinate system as in Lemma 4.13, the transformation

$$(26) \qquad \mathbf{B}_{e,i} = \begin{pmatrix} \kappa_e^{-i} & 0 & 0 \\ 0 & \kappa_e^{-i} & 0 \\ b_1\kappa_e^{-i} & b_2\kappa_e^{-i} & 2^i \end{pmatrix}$$

maps $T_{(i+1)}$ to some o-tetrahedron in $\hat{\mathcal{T}}_1$.

Case 2. $T_{(i+1)}$ is a child tetrahedron of a v_e-tetrahedron $T_{(i)} \in \mathcal{T}_i$. Let $T_{(k)} \in \mathcal{T}_k$, $1 \le k \le i$, be the v_e-tetrahedron, such that $T_{(i)} \subset T_{(k)}$ and $T_{(k)}$'s parent tetrahedron $T_{(k-1)} \in \mathcal{T}_{k-1}$ is an e-tetrahedron. Using the $T_{(k-1)}$-based local coordinate system as in Lemma 4.14, the transformation

$$(27) \qquad \mathbf{B}_{i,k} = \begin{pmatrix} \kappa_e^{-i+1} & 0 & 0 \\ 0 & \kappa_e^{-i+1} & 0 \\ b_1\kappa_e^{-i+1} & b_2\kappa_e^{-i+1} & 2^{k-1}\kappa_e^{k-i} \end{pmatrix}$$

maps $T_{(i+1)}$ to an o-tetrahedron in $\hat{\mathcal{T}}_2$. In both cases, $|b_1|, |b_2| \le C_0$, for $C_0 > 0$ depending on $T_{(0)}$ but not on i or k.

Proof. If $T_{(i+1)}$ is a child tetrahedron of an e-tetrahedron $T_{(i)} \in \mathcal{T}_i$, the matrix in (23) maps $T_{(i)}$ to $\hat{T}$, and maps $P_{e,i+1} \cap T_{(i)}$ to $\hat{P}_1$, where $P_{e,i+1}$ is the parallelogram cutting $T_{(0)}$ in the $(i+1)$st refinement (Definition 4.6) and $\hat{P}_1$ is the parallelogram cutting $\hat{T}$ in the first edge refinement (see Figure 4). Consequently, $T_{(i+1)}$ is translated to one of the four o-tetrahedra in $\hat{\mathcal{T}}_1$ by the same mapping.

For Case II, the transformation (25) maps $T_{(i)}$ to a v_e-tetrahedron in $\hat{\mathcal{T}}_1$. In addition, it maps $P_{e,i} \cap \bar{T}_{(i)}$ to $\hat{P}_1$, and $P_{e,i+1} \cap T_{(i)}$ to $\hat{P}_2$ (see Figure 4). Therefore, the same transformation maps $T_{(i+1)}$ to an o-tetrahedron in $\hat{\mathcal{T}}_2$ between $\hat{P}_1$ and $\hat{P}_2$. This completes the proof. $\qquad\square$

Each tetrahedron in $\mathcal{T}_{i+1}$ that belongs to layer $L_{e,i}$ falls into either Case I or Case II of Lemma 4.15. Thus, there is a linear transformation $\mathbf{B}$ (either $\mathbf{B}_{e,i}$ or $\mathbf{B}_{i,k}$) that maps $T_{(i+1)}$ to an o-tetrahedron in either $\hat{\mathcal{T}}_1$ or in $\hat{\mathcal{T}}_2$. We denote this o-tetrahedron by $\hat{T}_{(i+1)}$. It is clear that $\hat{T}_{(i+1)}$ belongs to a finite number of similarity classes determined by the o-tetrahedra in $\hat{\mathcal{T}}_1$ and $\hat{\mathcal{T}}_2$. Then, for $(x, y, z) \in T_{(i+1)}$, we have

$$(28) \qquad \mathbf{B}(x, y, z) = (\hat{x}, \hat{y}, \hat{z}) \in \hat{T}_{(i+1)}.$$

For a function v on $T_{(i+1)}$, we define $\hat{v}(\hat{x}, \hat{y}, \hat{z}) := v(x, y, z)$.

In the $(i+1)$st refinement, $0 \le i < n$, when the layer $L_{e,i}$ is formed, it only contains tetrahedra in $\mathcal{T}_{i+1}$. To obtain the mesh $\mathcal{T}_n$, these tetrahedra in $L_{e,i}$ are further refined uniformly $n - i - 1$ times. In the following, we obtain a uniform interpolation error estimate for the mesh $\mathcal{T}_n$ in the layer $L_{e,i}$.

Theorem 4.16. *Let $T_{(0)} \in \mathcal{T}_0$ be an e-tetrahedron. For $u \in \mathcal{M}_{a+1}^{m+1}(\Omega)$, where $\boldsymbol{a}$ is given in (14), let u_I be its nodal interpolation on $\mathcal{T}_n$. Then, for $0 \le i < n$, we have*

$$|u - u_I|_{H^1(L_{e,i})} \le C h^m \|u\|_{\mathcal{M}_{a+1}^{m+1}(L_{e,i})},$$

where $L_{e,i}$ is the mesh layer in Definition 4.6, $h = 2^{-n}$, and C depends on $T_{(0)}$ and m, but not on i.

Proof. Based on Algorithm 3.2, the layer $L_{e,i}$ is formed in the $(i+1)$st refinement and is the union of tetrahedra in $\mathcal{T}_{i+1}$ between $P_{e,i}$ and $P_{e,i+1}$. Therefore, it suffices to verify the following interpolation error estimate on each tetrahedron $\mathcal{T}_{i+1} \ni T_{(i+1)} \subset L_{e,i}$,

$$(29) \qquad |u - u_I|_{H^1(T_{(i+1)})} \le C h^m \|u\|_{\mathcal{M}_{a+1}^{m+1}(T_{(i+1)})}.$$

We show this estimate based on the type of $T_{(i+1)}$'s parent tetrahedron.

Case I. $T_{(i+1)}$'s parent is an e-tetrahedron in $\mathcal{T}_i$. Let $(x, y, z) \in T_{(i+1)}$ and $(\hat{x}, \hat{y}, \hat{z}) \in \hat{T}_{(i+1)}$ as in (28). Then, by the mapping in (26) and direct calculation, we have

$$(30) \quad \begin{cases} dx\,dy\,dz = 2^{-i}\kappa_e^{2i}\,d\hat{x}\,d\hat{y}\,d\hat{z}; \\ \partial_x v = (\kappa_e^{-i}\partial_{\hat{x}} + b_1\kappa_e^{-i}\partial_{\hat{z}})\hat{v}, \quad \partial_y v = (\kappa_e^{-i}\partial_{\hat{y}} + b_2\kappa_e^{-i}\partial_{\hat{z}})\hat{v}, \quad \partial_z v = 2^i\partial_{\hat{z}}\hat{v}; \\ \partial_{\hat{x}}\hat{v} = (\kappa_e^i\partial_x - b_1 2^{-i}\partial_z)v, \quad \partial_{\hat{y}}\hat{v} = (\kappa_e^i\partial_y - b_2 2^{-i}\partial_z)v, \quad \partial_{\hat{z}}\hat{v} = 2^{-i}\partial_z v. \end{cases}$$

Therefore, by Lemma 4.15, (30), the standard interpolation estimate on $\hat{T}_{(i+1)}$, (19), and (12), we have

$$\|\partial_x(u - u_I)\|_{L^2(T_{(i+1)})}^2 \le C 2^{-i}\big(\|\partial_{\hat{x}}(\hat{u} - \hat{u}_I)\|_{L^2(\hat{T}_{(i+1)})}^2 + \|\partial_{\hat{z}}(\hat{u} - \hat{u}_I)\|_{L^2(\hat{T}_{(i+1)})}^2\big)$$

$$\le C 2^{-i} 2^{2m(i-n)} |\hat{u}|_{H^{m+1}(\hat{T}_{(i+1)})}^2$$

$$\le C 2^{2m(i-n)} \sum_{|\alpha_\perp|+\alpha_3=m+1} 2^{-2i\alpha_3} \kappa_e^{2i(|\alpha_\perp|-1)} \|\partial^{\alpha_\perp}\partial_z^{\alpha_3} u\|_{L^2(T_{(i+1)})}^2$$

$$\le C 2^{2m(i-n)} \sum_{|\alpha_\perp|+\alpha_3=m+1} 2^{-2i\alpha_3} \|\rho_e^{|\alpha_\perp|-1}\partial^{\alpha_\perp}\partial_z^{\alpha_3} u\|_{L^2(T_{(i+1)})}^2$$

$$\le C 2^{2m(i-n)} \kappa_e^{2ia_e} \|u\|_{\mathcal{M}_{a+1}^{m+1}(T_{(i+1)})}^2 \le C h^{2m} \|u\|_{\mathcal{M}_{a+1}^{m+1}(T_{(i+1)})}^2.$$

A similar calculation for the derivative with respect to y gives

$$\|\partial_y(u - u_I)\|_{L^2(T_{(i+1)})} \le C h^m \|u\|_{\mathcal{M}_{a+1}^{m+1}(T_{(i+1)})}.$$

In the z-direction, by Lemma 4.15, (30), the standard interpolation estimate, (19), and (12), we have

$$
\begin{aligned}
\|\partial_z(u - u_I)\|^2_{L^2(T_{(i+1)})} &\leq C2^i \kappa_e^{2i} \|\partial_{\hat{z}}(\hat{u} - \hat{u}_I)\|^2_{L^2(\hat{T}_{(i+1)})} \\
&\leq C2^i \kappa_e^{2i} 2^{2m(i-n)} |\hat{u}|^2_{H^{m+1}(\hat{T}_{(i+1)})} \\
&\leq C2^{2m(i-n)} \sum_{|\alpha_\perp|+\alpha_3=m+1} 2^{2i} 2^{-2i\alpha_3} \kappa_e^{2i|\alpha_\perp|} \|\partial^{\alpha_\perp} \partial_z^{\alpha_3} u\|^2_{L^2(T_{(i+1)})} \\
&\leq C2^{2m(i-n)} \sum_{|\alpha_\perp|+\alpha_3=m+1} 2^{-2i\alpha_3} \|\rho_e^{|\alpha_\perp|-1} \partial^{\alpha_\perp} \partial_z^{\alpha_3} u\|^2_{L^2(T_{(i+1)})} \\
&\leq C2^{2m(i-n)} \kappa_e^{2ia_e} \|u\|^2_{\mathcal{M}_{a+1}^{m+1}(T_{(i+1)})} \leq Ch^{2m} \|u\|^2_{\mathcal{M}_{a+1}^{m+1}(T_{(i+1)})}.
\end{aligned}
$$

Hence, we have completed the proof for (29).

Case II. $T_{(i+1)}$'s parent is a v_e-tetrahedron $T_{(i)} \in \mathcal{T}_i$. Let $T_{(k)} \in \mathcal{T}_k$, $1 \leq k \leq i$, be the v_e-tetrahedron, such that $T_{(i)} \subset T_{(k)}$ and $T_{(k)}$'s parent tetrahedron $T_{(k-1)} \in \mathcal{T}_{k-1}$ is an e-tetrahedron. Then, using the mapping (27), by (28), for $(x, y, z) \in T_{(i+1)}$ and $(\hat{x}, \hat{y}, \hat{z}) \in \hat{T}_{(i+1)}$, we have

$$
(31) \quad
\begin{cases}
dx\,dy\,dz = 2^{1-k} \kappa_e^{3i-k-2} d\hat{x}\,d\hat{y}\,d\hat{z}; \\
\partial_x v = (\kappa_e^{1-i} \partial_{\hat{x}} + b_1 \kappa_e^{1-i} \partial_{\hat{z}})\hat{v}, \quad \partial_y v = (\kappa_e^{1-i} \partial_{\hat{y}} + b_2 \kappa_e^{1-i} \partial_{\hat{z}})\hat{v}, \\
\partial_z v = 2^{k-1} \kappa_e^{k-i} \partial_{\hat{z}} \hat{v}; \\
\partial_{\hat{x}} \hat{v} = (\kappa_e^{i-1} \partial_x - b_1 2^{1-k} \kappa_e^{i-k} \partial_z)v, \quad \partial_{\hat{y}} \hat{v} = (\kappa_e^{i-1} \partial_y - b_2 2^{1-k} \kappa_e^{i-k} \partial_z)v, \\
\partial_{\hat{z}} \hat{v} = 2^{1-k} \kappa_e^{i-k} \partial_z v.
\end{cases}
$$

Therefore, by Lemma 4.15, (31), the standard interpolation estimate, (19), and (12), we have

$$
\begin{aligned}
\|\partial_x(u - u_I)\|^2_{L^2(T_{(i+1)})} &\leq C2^{1-k} \kappa_e^{i-k} \left(\|\partial_{\hat{x}}(\hat{u} - \hat{u}_I)\|^2_{L^2(\hat{T}_{(i+1)})} + \|\partial_{\hat{z}}(\hat{u} - \hat{u}_I)\|^2_{L^2(\hat{T}_{(i+1)})} \right) \\
&\leq C2^{1-k} \kappa_e^{i-k} 2^{2m(i-n)} |\hat{u}|^2_{H^{m+1}(\hat{T}_{(i+1)})} \\
&\leq C2^{2m(i-n)} \sum_{|\alpha_\perp|+\alpha_3=m+1} 2^{2(1-k)\alpha_3} \kappa_e^{2(i-k)\alpha_3} \kappa_e^{(2i-2)(|\alpha_\perp|-1)} \|\partial^{\alpha_\perp} \partial_z^{\alpha_3} u\|^2_{L^2(T_{(i+1)})} \\
&\leq C2^{2m(i-n)} \sum_{|\alpha_\perp|+\alpha_3=m+1} 2^{2(1-k)\alpha_3} \|\rho_e^{|\alpha_\perp|-1} \partial^{\alpha_\perp} \partial_z^{\alpha_3} u\|^2_{L^2(T_{(i+1)})} \\
&\leq C2^{2m(i-n)} \kappa_e^{2ia_e} \|u\|^2_{\mathcal{M}_{a+1}^{m+1}(T_{(i+1)})} \leq Ch^{2m} \|u\|^2_{\mathcal{M}_{a+1}^{m+1}(T_{(i+1)})}.
\end{aligned}
$$

A similar calculation for the derivative with respect to y gives

$$
\|\partial_y(u - u_I)\|_{L^2(T_{(i+1)})} \leq Ch^m \|u\|_{\mathcal{M}_{a+1}^{m+1}(T_{(i+1)})}.
$$

In the z-direction, by Lemma 4.15, (31), the standard interpolation estimate, (19), and (12), we have

$$\|\partial_z(u - u_I)\|^2_{L^2(T_{(i+1)})} \leq C(2^{1-k}\kappa_e^{i-k})\kappa_e^{2(i-1)}(2^{k-1}\kappa_e^{k-i})^2\|\partial_{\hat{z}}(\hat{u} - \hat{u}_I)\|^2_{L^2(\hat{T}_{(i+1)})}$$

$$\leq C(2^{1-k}\kappa_e^{i-k})\kappa_e^{2(i-1)}(2^{k-1}\kappa_e^{k-i})^2 2^{2m(i-n)}|\hat{u}|^2_{H^{m+1}(\hat{T}_{(i+1)})}$$

$$\leq C2^{2m(i-n)}\sum_{|\alpha_\perp|+\alpha_3=m+1}(2^{1-k}\kappa_e^{i-k})^{2(\alpha_3-1)}\kappa_e^{2|\alpha_\perp|(i-1)}\|\partial^{\alpha_\perp}\partial_z^{\alpha_3}u\|^2_{L^2(T_{(i+1)})}$$

$$\leq C2^{2m(i-n)}\sum_{|\alpha_\perp|+\alpha_3=m+1}(2^{1-k}\kappa_e^{i-k})^{2(\alpha_3-1)}\kappa_e^{2i-2|\alpha_\perp|}\|\rho_e^{|\alpha_\perp|-1}\partial^{\alpha_\perp}\partial_z^{\alpha_3}u\|^2_{L^2(T_{(i+1)})}$$

$$\leq C2^{2m(i-n)}\kappa_e^{2ia_e}\|u\|^2_{\mathcal{M}^{m+1}_{a+1}(T_{(i+1)})} \leq Ch^{2m}\|u\|^2_{\mathcal{M}^{m+1}_{a+1}(T_{(i+1)})}.$$

This completes the proof for (29) of Case II.

Hence, the theorem is proved by summing up the estimates for all the tetrahedra $T_{(i+1)}$ in $L_{e,i}$. $\square$

Remark 4.17. The main ingredients for the proof of Theorem 4.16 include the scaling argument based on the mappings in Lemma 4.15 and the standard interpolation estimates. Despite the slight difference in the interpolation error analsyis for different directional derivatives, the calculations in the proof show that for the element $T_{(i+1)}$ away from the edge, we have

$$|u - u_I|_{H^1(T_{(i+1)})} \leq C2^{m(i-n)}h_\perp^{-1}\sum_{|\alpha|=m+1}h_\perp^{|\alpha_\perp|}h_3^{\alpha_3}\|\partial^\alpha u\|_{L^2(T_{(i+1)})},$$

where $h_\perp$ is the size of the projection of the element in the xy-plane, and h_3 is the size of the element along the edge direction. In the proof, $h_\perp$ and h_3 are replaced by specific expressions in terms of the grading parameters, such that they can be transferred to the proper weight in the norm.

Then, we extend the interpolation error estimate to the entire initial tetrahedron $T_{(0)} \in \mathcal{T}_0$.

Corollary 4.18. *Let* $T_{(0)} \in \mathcal{T}_0$ *be an e-tetrahedron. For* $u \in \mathcal{M}^{m+1}_{a+1}(\Omega)$, *where* $\boldsymbol{a}$ *is given in* (14), *let* u_I *be its nodal interpolation on* $\mathcal{T}_n$. *Then, we have*

$$|u - u_I|_{H^1(T_{(0)})} \leq Ch^m\|u\|_{\mathcal{M}^{m+1}_{a+1}(T_{(0)})},$$

where $h = 2^{-n}$ *and* C *depends on* $T_{(0)}$ *and* m.

Proof. By Theorem 4.16, it suffices to show the estimate for any tetrahedron $T_{(n)} \in \mathcal{T}_n$ in the last layer $L_{e,n}$. We derive the desired estimate in the following two cases.

Case I. $T_{(n)}$ is an e-tetrahedron. By Lemma 4.13, the mapping $\mathbf{B}_{e,n}$ translates $T_{(n)}$ to the reference tetrahedron $\hat{T}$. Consequently, it maps any point $(x, y, z) \in T_{(n)}$ to $(\hat{x}, \hat{y}, \hat{z}) \in \hat{T}$. For a function v on $T_{(n)}$, we define $\hat{v}$ on $\hat{T}$ by

$$\hat{v}(\hat{x}, \hat{y}, \hat{z}) := v(x, y, z).$$

Now, let χ be a smooth cutoff function on $\hat{T}$ such that $\chi = 0$ in a neighborhood of the edge $\hat{e} := \hat{x}_0\hat{x}_1$ and $= 1$ at every other Lagrange node of $\hat{T}$. Let $\rho_{\hat{e}}$ be the

distance to $\hat{e}$. Let $\hat{u}_I$ be the interpolation of $\hat{u}$ on the reference tetrahedron $\hat{T}$. Since $\chi\hat{u} = 0$ in the neighborhood of $\hat{e}$, $(\chi\hat{u})_I = \hat{u}_I$ and

$$
(32) \qquad |\chi\hat{u}|_{H^{m+1}(\hat{T})}^2 \le C \sum_{|\alpha_\perp| + \alpha_3 \le m+1} \|\rho_{\hat{e}}^{|\alpha_\perp|-1} \partial^{\alpha_\perp} \partial_{\hat{z}}^{\alpha_3} \hat{u}\|_{L^2(\hat{T})}^2.
$$

Define $\hat{w} := \hat{u} - \chi\hat{u}$. Then, by the usual interpolation error estimate, we have

$$
\begin{aligned}
|\hat{u} - \hat{u}_I|_{H^1(\hat{T})} &= |\hat{w} + \chi\hat{u} - \hat{u}_I|_{H^1(\hat{T})} \le |\hat{w}|_{H^1(\hat{T})} + |\chi\hat{u} - \hat{u}_I|_{H^1(\hat{T})} \\
(33) \qquad &= |\hat{w}|_{H^1(\hat{T})} + |\chi\hat{u} - (\chi\hat{u})_I|_{H^1(\hat{T})} \le C(\|\hat{u}\|_{H^1(\hat{T})} + |\chi\hat{u}|_{H^{m+1}(\hat{T})}),
\end{aligned}
$$

where C depends on m and, through χ, the nodes on $\hat{T}$. Then, using the scaling argument based on (30), (33), (32), the relation $\rho_{\hat{e}}(\hat{x}, \hat{y}, \hat{z}) = \kappa_e^{-n} \rho_e(x, y, z)$, and (12), we have

$$
\begin{aligned}
\|\partial_x(u - u_I)\|_{L^2(T_{(n)})}^2 &\le C 2^{-n} \left(\|\partial_{\hat{x}}(\hat{u} - \hat{u}_I)\|_{L^2(\hat{T})}^2 + \|\partial_{\hat{z}}(\hat{u} - \hat{u}_I)\|_{L^2(\hat{T})}^2 \right) \\
&\le C 2^{-n} \sum_{|\alpha_\perp| + \alpha_3 \le m+1} \|\rho_{\hat{e}}^{|\alpha_\perp|-1} \partial^{\alpha_\perp} \partial_{\hat{z}}^{\alpha_3} \hat{u}\|_{L^2(\hat{T})}^2 \\
&\le C \sum_{|\alpha_\perp| + \alpha_3 \le m+1} 2^{-2n\alpha_3} \|\rho_e^{|\alpha_\perp|-1} \partial^{\alpha_\perp} \partial_z^{\alpha_3} u\|_{L^2(T_{(n)})}^2 \\
&\le C \sum_{|\alpha_\perp| + \alpha_3 \le m+1} 2^{-2n\alpha_3} \kappa_e^{2na_e} \|\rho_e^{|\alpha_\perp|-1-a_e} \partial^{\alpha_\perp} \partial_z^{\alpha_3} u\|_{L^2(T_{(n)})}^2 \\
&\le C h^{2m} \|u\|_{\mathcal{M}_{a+1}^{m+1}(T_{(n)})}^2.
\end{aligned}
$$

A similar calculation for the derivative with respect to y gives

$$
\|\partial_y(u - u_I)\|_{L^2(T_{(n)})} \le C h^m \|u\|_{\mathcal{M}_{a+1}^{m+1}(T_{(n)})}.
$$

In the z-direction, using (33), (32), (30), and (12), we have

$$
\begin{aligned}
\|\partial_z(u - u_I)\|_{L^2(T_{(n)})}^2 &= 2^n \kappa_e^{2n} \|\partial_{\hat{z}}(\hat{u} - \hat{u}_I)\|_{L^2(\hat{T})}^2 \\
&\le C 2^n \kappa_e^{2n} \sum_{|\alpha_\perp| + \alpha_3 \le m+1} \|\rho_{\hat{e}}^{|\alpha_\perp|-1} \partial^{\alpha_\perp} \partial_{\hat{z}}^{\alpha_3} \hat{u}\|_{L^2(\hat{T})}^2 \\
&\le C \sum_{|\alpha_\perp| + \alpha_3 \le m+1} 2^{-2n\alpha_3} \|\rho_e^{|\alpha_\perp|-1} \partial^{\alpha_\perp} \partial_z^{\alpha_3} u\|_{L^2(T_{(n)})}^2 \\
&\le C \kappa_e^{2na_e} \|u\|_{\mathcal{M}_{a+1}^{m+1}(T_{(n)})}^2 \le C h^{2m} \|u\|_{\mathcal{M}_{a+1}^{m+1}(T_{(n)})}^2.
\end{aligned}
$$

Thus, we have proved the estimate for Case I.

Case II. $T_{(n)}$ is a v_e-tetrahedron. Let $T_{(k)} \in \mathcal{T}_k$, $1 \le k \le n$, be the v_e-tetrahedron, such that $T_{(n)} \subset T_{(k)}$ and $T_{(k)}$'s parent tetrahedron $T_{(k-1)} \in \mathcal{T}_{k-1}$ is an e-tetrahedron. By Lemma 4.14, the mapping $\mathbf{B}_{n,k}$ translates $T_{(n)}$ to a v_e-tetrahedron in $\hat{T}_{(n)} \in \hat{\mathcal{T}}_1$. Thus, $\mathbf{B}_{n,k}$ maps every point $(x, y, z) \in T_{(n)}$ to $(\hat{x}, \hat{y}, \hat{z}) \in \hat{T}_{(n)}$. As in Case I, for a function v on $T_{(n)}$, we define $\hat{v}$ on $\hat{T}_{(n)}$ by

$$
\hat{v}(\hat{x}, \hat{y}, \hat{z}) := v(x, y, z).
$$

Now let χ be a smooth cutoff function on $\hat{T}_{(n)}$ such that $\chi = 0$ in a neighborhood of the singular vertex on $\hat{e} := \hat{x}_0 \hat{x}_1$ of $\hat{T}$ and $= 1$ at every other Lagrange node of

$\hat{T}_{(n)}$. Recall the distance $\rho_{\hat{e}}$ to $\hat{e}$. Since $\chi\hat{u} = 0$ in the neighborhood of the singular vertex, we have $(\chi\hat{u})_I = \hat{u}_I$ on $\hat{T}_{(n)}$ and

$$(34) \qquad |\chi\hat{u}|^2_{H^{m+1}(\hat{T}_{(n)})} \le C \sum_{|\alpha_\perp|+\alpha_3 \le m+1} \|\rho_{\hat{e}}^{|\alpha_\perp|-1} \partial^{\alpha_\perp} \partial_{\hat{z}}^{\alpha_3} \hat{u}\|^2_{L^2(\hat{T}_{(n)})}.$$

Define $\hat{w} := \hat{u} - \chi\hat{u}$. Then, by the usual interpolation error estimate, we have

$$
\begin{aligned}
|\hat{u} - \hat{u}_I|_{H^1(\hat{T}_{(n)})} &= |\hat{w} + \chi\hat{u} - \hat{u}_I|_{H^1(\hat{T}_{(n)})} \le |\hat{w}|_{H^1(\hat{T}_{(n)})} + |\chi\hat{u} - \hat{u}_I|_{H^1(\hat{T}_{(n)})} \\
(35) \qquad &= |\hat{w}|_{H^1(\hat{T}_{(n)})} + |\chi\hat{u} - (\chi\hat{u})_I|_{H^1(\hat{T}_{(n)})} \\
&\le C(\|\hat{u}\|_{H^1(\hat{T}_{(n)})} + |\chi\hat{u}|_{H^{m+1}(\hat{T}_{(n)})}),
\end{aligned}
$$

where C depends on m and, through χ, the nodes in the $\hat{T}_{(n)}$. In $L_{e,n}$, $\rho_e(x,y,z) = \kappa_e^{n-1}\rho_{\hat{e}}(\hat{x},\hat{y},\hat{z})$. Therefore, by (31), (35), (34), and (12), we have

$$
\begin{aligned}
\|\partial_x(u - u_I)\|^2_{L^2(T_{(n)})} &\le C2^{1-k}\kappa_e^{n-k}\left(\|\partial_{\hat{x}}(\hat{u} - \hat{u}_I)\|^2_{L^2(\hat{T}_{(n)})} + \|\partial_{\hat{z}}(\hat{u} - \hat{u}_I)\|^2_{L^2(\hat{T}_{(n)})}\right) \\
&\le C2^{1-k}\kappa_e^{n-k} \sum_{|\alpha_\perp|+\alpha_3 \le m+1} \|\rho_{\hat{e}}^{|\alpha_\perp|-1} \partial^{\alpha_\perp} \partial_{\hat{z}}^{\alpha_3} \hat{u}\|^2_{L^2(\hat{T}_{(n)})} \\
&\le C \sum_{|\alpha_\perp|+\alpha_3 \le m+1} 2^{2(1-k)\alpha_3} \kappa_e^{2(n-k)\alpha_3} \|\rho_e^{|\alpha_\perp|-1} \partial^{\alpha_\perp} \partial_z^{\alpha_3} u\|^2_{L^2(T_{(n)})} \\
&\le C\kappa_e^{2na_e} \|u\|^2_{\mathcal{M}^{m+1}_{a+1}(T_{(n)})} \le Ch^{2m}\|u\|^2_{\mathcal{M}^{m+1}_{a+1}(T_{(n)})}.
\end{aligned}
$$

A similar calculation for the derivative with respect to y gives

$$\|\partial_y(u - u_I)\|_{L^2(T_{(n)})} \le Ch^m \|u\|_{\mathcal{M}^{m+1}_{a+1}(T_{(n)})}.$$

In the z-direction, by (31), (35), (34), and (12), we have

$$
\begin{aligned}
\|\partial_z(u - u_I)\|^2_{L^2(T_{(n)})} &= (2^{1-k}\kappa_e^{n-k})\kappa_e^{2(n-1)}(2^{k-1}\kappa_e^{k-n})^2\|\partial_{\hat{z}}(\hat{u} - \hat{u}_I)\|^2_{L^2(\hat{T}_{(n)})} \\
&\le C(2^{1-k}\kappa_e^{n-k})\kappa_e^{2(n-1)}(2^{k-1}\kappa_e^{k-n})^2 \sum_{|\alpha_\perp|+\alpha_3 \le m+1} \|\rho_{\hat{e}}^{|\alpha_\perp|-1} \partial^{\alpha_\perp} \partial_{\hat{z}}^{\alpha_3} \hat{u}\|^2_{L^2(\hat{T}_{(n)})} \\
&\le C \sum_{|\alpha_\perp|+\alpha_3 \le m+1} (2^{1-k}\kappa_e^{n-k})^{2\alpha_3}(2^{k-1}\kappa_e^k)^2 \|\rho_e^{|\alpha_\perp|-1} \partial^{\alpha_\perp} \partial_z^{\alpha_3} u\|^2_{L^2(T^{(n)})} \\
&\le C\kappa_e^{2na_e} \|u\|^2_{\mathcal{M}^{m+1}_{a+1}(T_{(n)})} \le Ch^{2m}\|u\|^2_{\mathcal{M}^{m+1}_{a+1}(T_{(n)})}.
\end{aligned}
$$

Thus, we have proved the estimate for Case II.

Hence, the corollary is proved by summing up the estimates in Theorem 4.16 and the estimates for all the tetrahedra $T_{(n)}$ in $L_{e,n}$. $\qquad\square$

4.3. Estimates on initial ev-tetrahedra in $\mathcal{T}_0$.

In this subsection, we denote by $T_{(0)} = \triangle^4 x_0 x_1 x_2 x_3 \in \mathcal{T}_0$ an ev-tetrahedron, such that $x_0 = v \in \mathcal{V}$ and $x_0 x_1$ is on the edge $e \in \mathcal{E}$. Then, we first define mesh layers associated with $\mathcal{T}_n$ on $T_{(0)}$.

Definition 4.19 (Mesh layers in ev-tetrahedra). For $1 \le i \le n$, the ith refinement on $T_{(0)}$ produces a small tetrahedron with x_0 as a vertex. We denote by $P_{ev,i}$ the face of this small tetrahedron whose closure does not contain x_0 (see the last two pictures in Figure 1). Then, for the mesh $\mathcal{T}_n$ on $T_{(0)}$, we define the ith mesh layer $L_{ev,i}$, $1 \le i < n$, as the region in $T_{(0)}$ between $P_{ev,i}$ and $P_{ev,i+1}$. We denote by $L_{ev,0}$ the region in $T_{(0)}$ between $\triangle^3 x_1 x_2 x_3$ and $P_{ev,1}$ and let $L_{ev,n} \subset T_{(0)}$ be the small tetrahedron with x_0 as a vertex that is generated in the nth refinement.

For each ev-tetrahedron, one extra refinement results in one ev-tetrahedron, one e-tetrahedron, two v_e-tetrahedra, and four o-tetrahedra. Let $T = \triangle^4\gamma_0\gamma_1\gamma_2\gamma_3 \subset T_{(0)}$ be an ev-tetrahedron generated by some subsequent refinements of $T_{(0)}$, with $\gamma_0 = x_0$ and $\gamma_0\gamma_1$ on the edge $e \in \mathcal{E}$. We define the relative distances $c_{\gamma,1}$ and $c_{\gamma,2}$ for T using the same notation as in Definition 4.8 (see also Remark 4.10). In the next lemma, we show the analogue of Lemma 4.11 for ev-tetrahedra. Namely, the relative distances are bounded for ev-tetrahedra with respect to the refinement.

Lemma 4.20. *Let $T = \triangle^4\gamma_0\gamma_1\gamma_2\gamma_3 \subset T_{(0)}$ be an ev-tetrahedron in $\mathcal{T}_i$, $1 \le i < n$, with $\gamma_0 = x_0$ and $\gamma_0\gamma_1$ on the edge $e \in \mathcal{E}$. Let $T_R \subset T$ be the ev-tetrahedron in $\mathcal{T}_{i+1}$. Denote by c_T and c_R the absolute distances (22) for T and T_R, respectively. Then, $c_R \le \max(c_T, 1)$.*

Proof. Recall the grading parameters κ_v, κ_e, and κ_{ev} for $T_{(0)}$ with $\kappa_v, \kappa_e \ge \kappa_{ev}$. We use Figure 3 to demonstrate the proof. Then, $T_R = \triangle^4\gamma_0\gamma_4\gamma_5\gamma_6$. Consider the triangles on the face $\triangle^3\gamma_0\gamma_1\gamma_2$ of T, induced by the sub-tetrahedra after one refinement on T, where γ_5' and γ_2' are the orthogonal projections of γ_5 and γ_2 on the singular edge. However, note that instead of the mid-point of $\gamma_0\gamma_1$ for the e-tetrahedron, the location of γ_4 here is given by $|\gamma_0\gamma_4| = \kappa_v|\gamma_0\gamma_1|$ for the ev-tetrahedron. Let $c_{\gamma_2,1}, c_{\gamma_2,2}$ (resp. $c_{\gamma_5,1}^R, c_{\gamma_5,2}^R$) be the relative distances of γ_2 in T (resp. γ_5 in T_R).

Based on Algorithm 3.2, $|\gamma_0\gamma_5'| = \kappa_{ev}|\gamma_0\gamma_2'|$. By (20), $c_{\gamma_5,1}^R$ and $c_{\gamma_2,1}$ have the same sign. Then, we first show $|c_{\gamma_5,1}^R|, |c_{\gamma_5,2}^R| \le \max(|c_{\gamma_2,1}|, |c_{\gamma_2,2}|, 1)$ by considering the following cases, in which the calculations are based on the definitions in (20) and (21).

If $c_{\gamma_2,1} < 0$, we have

$$0 > c_{\gamma_5,1}^R = -|\gamma_0\gamma_5'|/|\gamma_0\gamma_4| = -\kappa_v^{-1}\kappa_{e,v}|\gamma_0\gamma_2'|/|\gamma_0\gamma_1| = \kappa_v^{-1}\kappa_{ev}c_{\gamma_2,1} \ge c_{\gamma_2,1}.$$

Therefore, $|c_{\gamma_5,1}^R| \le |c_{\gamma_2,1}|$. Meanwhile, we have

$$1 \le c_{\gamma_5,2}^R = 1 - c_{\gamma_5,1}^R = 1 - \kappa_v^{-1}\kappa_{ev}c_{\gamma_2,1} < 1 - c_{\gamma_2,1} = c_{\gamma_2,2}.$$

Therefore, $|c_{\gamma_5,2}^R| \le |c_{\gamma_2,2}|$.

If $0 \le c_{\gamma_2,1} < \kappa_v\kappa_{ev}^{-1}$, we have $c_{\gamma_5,1}^R \ge 0$ and

$$c_{\gamma_5,1}^R = |\gamma_0\gamma_5'|/|\gamma_0\gamma_4| = \kappa_v^{-1}\kappa_{ev}|\gamma_0\gamma_2'|/|\gamma_0\gamma_4| = \kappa_v^{-1}\kappa_{ev}c_{\gamma_2,1} < 1.$$

Meanwhile, we have

$$0 \le c_{\gamma_5,2}^R = 1 - c_{\gamma_5,1}^R \le 1.$$

If $c_{\gamma_2,1} \ge \kappa_v\kappa_{ev}^{-1}$, we have

$$1 \le c_{\gamma_5,1}^R = |\gamma_0\gamma_5'|/|\gamma_0\gamma_4| = \kappa_v^{-1}\kappa_{ev}|\gamma_0\gamma_2'|/|\gamma_0\gamma_4| = \kappa_v^{-1}\kappa_{ev}c_{\gamma_2,1} \le |c_{\gamma_2,1}|.$$

Meanwhile, we have

$$0 \ge c_{\gamma_5,2}^R = 1 - c_{\gamma_5,1}^R = 1 - \kappa_v^{-1}\kappa_{ev}c_{\gamma_2,1} \ge 1 - c_{\gamma_2,1} = c_{\gamma_2,2}.$$

Therefore, $|c_{\gamma_5,2}^R| \le |c_{\gamma_2,2}|$.

Hence, $|c_{\gamma_5,1}^R|, |c_{\gamma_5,2}^R| \le \max(|c_{\gamma_2,1}|, |c_{\gamma_2,2}|, 1)$. Using a similar calculation, we can also obtain the same estimate for relative distances of γ_3 and γ_6. Then, the proof is completed by combining these estimates and by the definition of the absolute distance (22). $\square$

Now, we define the reference element for the ev-tetrahedron.

Definition 4.21 (The reference *ev*-tetrahedron). We shall use the tetrahedron $\hat{T} = \triangle^4 \hat{x}_0 \hat{x}_1 \hat{x}_2 \hat{x}_3$ in Definition 4.12 as our reference element in this subsection. For $T_{(0)}$, recall the grading parameters κ_v and κ_e associated with x_0 and $x_0 x_1$, respectively. For the reference *ev*-tetrahedron $\hat{T}$, one graded refinement using the same parameters κ_v, κ_e, and κ_{ev} for $\hat{x}_0$ and $\hat{x}_0 \hat{x}_1$ gives rise to a triangulation on $\hat{T}$, which we denote by $\hat{\mathcal{T}}_1$. Define the union of the seven tetrahedra in $\hat{\mathcal{T}}_1$ away from $\hat{x}_0$ to be the mesh layer $\hat{L}$ on $\hat{T}$. We denote by $\hat{\mathcal{L}}$ the initial triangulation of $\hat{L}$ that contains these seven tetrahedra.

Then, we construct a mapping from an *ev*-tetrahedron $T \subset T_{(0)}$ in $\mathcal{T}_i$ to $\hat{T}$.

Lemma 4.22. *For an ev-tetrahedron $T := \triangle^4 \gamma_0 \gamma_1 \gamma_2 \gamma_3 \subset T_{(0)}$ in $\mathcal{T}_i$, $0 \le i \le n$, suppose $\gamma_0 = v \in \mathcal{V}$ and $\gamma_0 \gamma_1 \subset e \in \mathcal{E}$. Use a local Cartesian coordinate system, such that $(\gamma_0 + \gamma_1)/2$ is the origin, γ_1 is in the positive z-axis, and γ_2 is in the xz-plane. Then, there is a mapping*

$$(36) \qquad \mathbf{B}_{ev,i} = \begin{pmatrix} \kappa_{ev}^{-i} & 0 & 0 \\ 0 & \kappa_{ev}^{-i} & 0 \\ b_1 \kappa_{ev}^{-i} & b_2 \kappa_{ev}^{-i} & \kappa_v^{-i} \end{pmatrix}$$

with $|b_1|, |b_2| \le C_0$, for $C_0 \ge 0$ depending on $T_{(0)}$, such that $\mathbf{B}_{ev,i} : T \to \hat{T}$ is a bijection.

Proof. Recall $\hat{\lambda}_k$ and $\hat{\xi}_k$, $k = 2, 3$, in Definition 4.12. Based on Algorithm 3.2, we have $\gamma_2 = (\kappa_{ev}^i \hat{\lambda}_2, 0, \zeta_2)$, $\gamma_3 = (\kappa_{ev}^i \hat{\lambda}_3, \kappa_{ev}^i \hat{\xi}_3, \zeta_3)$, and $|\gamma_0 \gamma_1| = \kappa_v^i l_0 = \kappa_v^i |x_0 x_1|$, where ζ_2 and ζ_3 are the z-coordinates of the vertices γ_2 and γ_3, respectively. Then, the transformation

$$\mathbf{A}_1 := \begin{pmatrix} \kappa_{ev}^{-i} & 0 & 0 \\ 0 & \kappa_{ev}^{-i} & 0 \\ 0 & 0 & \kappa_v^{-i} \end{pmatrix}$$

maps T to a tetrahedron, with vertices $\mathbf{A}_1 \gamma_0 = (0, 0, -l_0/2)$, $\mathbf{A}_1 \gamma_1 = (0, 0, l_0/2)$, $\mathbf{A}_1 \gamma_2 = (\hat{\lambda}_2, 0, \kappa_v^{-i} \zeta_2)$, and $\mathbf{A}_1 \gamma_3 = (\hat{\lambda}_3, \hat{\xi}_3, \kappa_v^{-i} \zeta_3)$. Now, let

$$b_1 = -(\kappa_v^{-i} \zeta_2 + l_0/2)/\hat{\lambda}_2, \qquad b_2 = [\kappa_v^{-i}(\zeta_2 \hat{\lambda}_3 - \hat{\lambda}_2 \zeta_3) + l_0(\hat{\lambda}_3 - \hat{\lambda}_2)/2]/\hat{\lambda}_2 \hat{\xi}_3.$$

Define

$$\mathbf{A}_2 := \begin{pmatrix} 1 & 0 & 0 \\ 0 & 1 & 0 \\ b_1 & b_2 & 1 \end{pmatrix}.$$

By Lemma 4.20, the absolute distance for T is bounded by a constant determined by $T_{(0)}$. Therefore, we have $|\zeta_2|, |\zeta_3| \le C|\gamma_0 \gamma_1| = C\kappa_v^i l_0$, where C depends on the shape regularity of $T_{(0)}$. In addition, since $\hat{\lambda}_2, \hat{\lambda}_3, \hat{\xi}_3$ all depend on the shape regularity of $T^{(0)}$ and $\hat{\lambda}_2, \hat{\xi}_3 \ne 0$, the transformation

$$\mathbf{B}_{ev,i} := \mathbf{A}_2 \mathbf{A}_1 = \begin{pmatrix} \kappa_{ev}^{-i} & 0 & 0 \\ 0 & \kappa_{ev}^{-i} & 0 \\ b_1 \kappa_{ev}^{-i} & b_2 \kappa_{ev}^{-i} & \kappa_v^{-i} \end{pmatrix}$$

maps T to $\hat{T}$ with $|b_1|, |b_2| \le C_0$, where $C_0 \ge 0$ depends on $T_{(0)}$ but not on i. This completes the proof. $\qquad\square$

Using the mapping in Lemma 4.22, we present the interpolation error estimate in the mesh layer $L_{ev,i}$.

Theorem 4.23. *Let $T_{(0)} = \triangle^4 x_0 x_1 x_2 x_3 \in \mathcal{T}_0$ be an ev-tetrahedron defined above. Let $L_{ev,i}$ be the mesh layer in Definition 4.19, $0 \leq i < n$. Recall the parameters a_v, a_e, and a_{ev} associated to κ_v, κ_e, and κ_{ev} in (11)–(13). Define*

$$(37) \qquad a_V := (m+1)(1 - a_v^{-1} a_{ev}) + a_{ev}.$$

Suppose

$$\sum_{|\alpha_\perp| + \alpha_3 \leq m+1} \|\rho_v^{\alpha_3 - a_V + a_e} \rho_e^{|\alpha_\perp| - 1 - a_e} \partial^{\alpha_\perp} \partial_z^{\alpha_3} u\|_{L^2(T_{(0)})}^2 < \infty.$$

Let u_I be the nodal interpolation on $\mathcal{T}_n$. Then, we have

$$|u - u_I|_{H^1(L_{ev,i})}^2 \leq C h^{2m} \sum_{|\alpha_\perp| + \alpha_3 \leq m+1} \|\rho_v^{\alpha_3 - a_V + a_e} \rho_e^{|\alpha_\perp| - 1 - a_e} \partial^{\alpha_\perp} \partial_z^{\alpha_3} u\|_{L^2(L_{ev,i})}^2,$$

where $h = 2^{-n}$ and C depends on $T_{(0)}$ and m.

Proof. Let $T_{(i)} \subset T_{(0)}$ be the *ev*-tetrahedron in $\mathcal{T}_i$. Then by Definition 4.19, we have $L_{ev,i} = T_{(i)} \setminus T_{(i+1)}$. Then, the mapping $\mathbf{B}_{ev,i}$ in (36) translates $L_{ev,i}$ to $\hat{L}$ (see Definition 4.21). For a point $(x, y, z) \in L_{ev,i}$, let $(\hat{x}, \hat{y}, \hat{z}) \in \hat{L}$ be its image under $\mathbf{B}_{ev,i}$. For a function v on $L_{ev,i}$, define the function $\hat{v}$ on $\hat{L}$ by

$$\hat{v}(\hat{x}, \hat{y}, \hat{z}) := v(x, y, z).$$

Let $\rho_{\hat{e}}$ be the distance to $\hat{x}_0 \hat{x}_1$ on the reference tetrahedron $\hat{T}$. Then, it is clear that $\rho_e(x, y, z) = \kappa_{ev}^i \rho_{\hat{e}}(\hat{x}, \hat{y}, \hat{z})$ on $L_{ev,i}$. Meanwhile, $\mathbf{B}_{ev,i}$ maps the triangulation $\mathcal{T}_n$ on $L_{ev,i}$ to a graded triangulation on $\hat{L}$ that is obtained after $i + 1 - n$ refinements of the initial mesh $\hat{\mathcal{L}}$. Note that the subsequent refinements on $\hat{\mathcal{L}}$ are anisotropic with the parameter κ_e toward $\hat{x}_0 \hat{x}_1$, since $\hat{\mathcal{L}}$ does not contain *ev*- or *v*-tetrahedra.

Then, by the mapping (36), the scaling argument, Corollary 4.18, (19), and (12), we have

$$\|\partial_x(u - u_I)\|_{L^2(L_{ev,i})}^2 \leq C \kappa_v^i \big(\|\partial_{\hat{x}}(\hat{u} - \hat{u}_I)\|_{L^2(\hat{L})}^2 + \|\partial_{\hat{z}}(\hat{u} - \hat{u}_I)\|_{L^2(\hat{L})}^2 \big)$$

$$\leq C \kappa_v^i 2^{2m(i-n)} \sum_{|\alpha_\perp| + \alpha_3 \leq m+1} \|\rho_{\hat{e}}^{|\alpha_\perp| - 1 - a_e} \partial^{\alpha_\perp} \partial_{\hat{z}}^{\alpha_3} \hat{u}\|_{L^2(\hat{L})}^2$$

$$\leq C 2^{2m(i-n)} \sum_{|\alpha_\perp| + \alpha_3 \leq m+1} \kappa_v^{2i\alpha_3} \kappa_{ev}^{2ia_e} \|\rho_e^{|\alpha_\perp| - 1 - a_e} \partial^{\alpha_\perp} \partial_z^{\alpha_3} u\|_{L^2(L_{ev,i})}^2$$

$$(38) \qquad \leq C 2^{-2mn} \sum_{|\alpha_\perp| + \alpha_3 \leq m+1} 2^{2im} \kappa_v^{2i\alpha_3} \kappa_{ev}^{2ia_e} \|\rho_e^{|\alpha_\perp| - 1 - a_e} \partial^{\alpha_\perp} \partial_z^{\alpha_3} u\|_{L^2(L_{ev,i})}^2.$$

Note that $\kappa_{ev}^i \lesssim \rho_v \lesssim \kappa_v^i$ on $L_{ev,i}$, $a_v, a_e \geq a_{ev}$ (see (13)) and $a_V \geq a_v$. Then, we consider all the possible cases below.

(I) $(\alpha_3 \leq a_v.)$ Then, we have

$$\kappa_v^{i(\alpha_3 - a_v)} \lesssim \rho_v^{\alpha_3 - a_v}.$$

Then, by (11), we have

$$(39) \qquad 2^{im} \kappa_v^{i\alpha_3} \kappa_{ev}^{ia_e} \lesssim \rho_v^{\alpha_3 - a_v} \kappa_{ev}^{ia_e} \lesssim \rho_v^{\alpha_3 - a_v + a_e}.$$

(II) $((1 - a_v^{-1}a_{ev})(m + 1) < \alpha_3 \leq m + 1.)$ Note that $0 < a_v \leq m$. Therefore, by (13), we have

$$\kappa_v^{i\alpha_3} = 2^{-im\alpha_3/a_v} \leq 2^{-im\alpha_3/a_{ev}+ima_V/a_{ev}-im} = \kappa_{ev}^{i(\alpha_3-a_V+a_{ev})}.$$

Note that $\alpha_3 - a_V + a_{ev} > 0$, therefore,

$$(40) \qquad 2^{im}\kappa_v^{i\alpha_3}\kappa_{ev}^{ia_e} \leq 2^{im}\kappa_{ev}^{i(\alpha_3-a_V+a_{ev})}\kappa_{ev}^{ia_e} \lesssim \rho_v^{\alpha_3-a_V+a_e}.$$

(III) $(a_v < \alpha_3 \leq (1-a_v^{-1}a_{ev})(m+1).)$ If $a_{ev} = a_v$, we have $(1-a_v^{-1}a_{ev})(m+1) = 0$, and therefore such α_3 does not exist. Thus, we only need to consider the case $a_{ev} < a_v$. Note that $\alpha_3 - a_V + a_{ev} \leq 0$ and $a_{ev} \leq a_e$. Therefore, by (13), we have

$$(41) \qquad 2^{im}\kappa_v^{i\alpha_3}\kappa_{ev}^{ia_e} = \kappa_v^{i\alpha_3}\kappa_{ev}^{i(a_e-a_{ev})} \lesssim \rho_v^{\alpha_3-a_V+a_{ev}}\rho_v^{(a_e-a_{ev})} = \rho_v^{\alpha_3-a_V+a_e}.$$

Therefore, choosing a_V as in (37), by (38) – (41), we have shown that

$$(42) \qquad \|\partial_x(u - u_I)\|_{L^2(L_{ev,i})}^2$$
$$\leq C2^{-2mn} \sum_{|\alpha_\perp|+\alpha_3\leq m+1} \|\rho_v^{\alpha_3-a_V+a_e}\rho_e^{|\alpha_\perp|-1-a_e}\partial^{\alpha_\perp}\partial_z^{\alpha_3}u\|_{L^2(L_{ev,i})}^2.$$

In the y-direction, with a similar process, we obtain

$$(43) \qquad \|\partial_y(u - u_I)\|_{L^2(L_{ev,i})}^2$$
$$\leq C2^{-2mn} \sum_{|\alpha_\perp|+\alpha_3\leq m+1} \|\rho_v^{\alpha_3-a_V+a_e}\rho_e^{|\alpha_\perp|-1-a_e}\partial^{\alpha_\perp}\partial_z^{\alpha_3}u\|_{L^2(L_{ev,i})}^2.$$

In the z-direction, by the mapping (36), the scaling argument, and Corollary 4.18, we have

$$\|\partial_z(u - u_I)\|_{L^2(L_{ev,i})}^2 = \kappa_v^{-i}\kappa_{ev}^{2i}\|\partial_{\hat{z}}(\hat{u} - \hat{u}_I)\|_{L^2(\hat{L})}^2$$
$$\leq C2^{2m(i-n)}\kappa_v^{-i}\kappa_{ev}^{2i} \sum_{|\alpha_\perp|+\alpha_3\leq m+1} \|\rho_{\hat{e}}^{|\alpha_\perp|-1-a_e}\partial^{\alpha_\perp}\partial_{\hat{z}}^{\alpha_3}\hat{u}\|_{L^2(\hat{L})}^2$$
$$\leq C2^{-2mn} \sum_{|\alpha_\perp|+\alpha_3\leq m+1} 2^{2im}\kappa_v^{2i(\alpha_3-1)}\kappa_{ev}^{2i(1+a_e)}\|\rho_e^{|\alpha_\perp|-1-a_e}\partial^{\alpha_\perp}\partial_z^{\alpha_3}u\|_{L^2(L_{ev,i})}^2$$
$$\leq C2^{-2mn} \sum_{|\alpha_\perp|+\alpha_3\leq m+1} 2^{2im}\kappa_v^{2i\alpha_3}\kappa_{ev}^{2ia_e}\|\rho_e^{|\alpha_\perp|-1-a_e}\partial^{\alpha_\perp}\partial_z^{\alpha_3}u\|_{L^2(L_{ev,i})}^2$$
$$(44) \qquad \leq C2^{-2mn} \sum_{|\alpha_\perp|+\alpha_3\leq m+1} \|\rho_v^{\alpha_3-a_V+a_e}\rho_e^{|\alpha_\perp|-1-a}\partial^{\alpha_\perp}\partial_z^{\alpha_3}u\|_{L^2(L_{ev,i})}^2,$$

where the last inequality follows from the analysis in (39)–(41).

Hence, the proof is completed by the estimates in (42)–(44). $\qquad\qquad\square$

Then, we are ready to obtain the interpolation error estimate on the entire ev-tetrahedron $T_{(0)}$.

Corollary 4.24. *Let $T_{(0)} \in \mathcal{T}_0$ be an ev-tetrahedron as in Theorem 4.23. Recall a_V from (37). Suppose*

$$\sum_{|\alpha_\perp|+\alpha_3\leq m+1} \|\rho_v^{\alpha_3-a_V+a_e}\rho_e^{|\alpha_\perp|-1-a_e}\partial^{\alpha_\perp}\partial_z^{\alpha_3}u\|_{L^2(T_{(0)})}^2 < \infty.$$

Let u_I be the nodal interpolation on $\mathcal{T}_n$. Then, we have

$$|u - u_I|_{H^1(T_{(0)})}^2 \leq Ch^{2m} \sum_{|\alpha_\perp|+\alpha_3\leq m+1} \|\rho_v^{\alpha_3-a_V+a_e}\rho_e^{|\alpha_\perp|-1-a_e}\partial^{\alpha_\perp}\partial_z^{\alpha_3}u\|_{L^2(T_{(0)})}^2,$$

where $h = 2^{-n}$ and C depends on $T_{(0)}$ and m.

Proof. By Theorem 4.23, it suffices to show

$$|u - u_I|^2_{H^1(L_{ev,n})} \leq C2^{-2mn} \sum_{|\alpha_\perp|+\alpha_3 \leq m+1} \|\rho_v^{\alpha_3 - a_V + a_e} \rho_e^{|\alpha_\perp|-1-a_e} \partial^{\alpha_\perp} \partial_z^{\alpha_3} u\|^2_{L^2(L_{ev,n})}.$$

By Lemma 4.22, $\mathbf{B}_{ev,n}(L_{ev,n}) = \hat{T}$. For $(x, y, z) \in L_{ev,n}$, let $(\hat{x}, \hat{y}, \hat{z}) \in \hat{T}$ be its image under $\mathbf{B}_{ev,n}$. For a function v on $L_{ev,n}$, we define $\hat{v}$ on $\hat{T}$ by

$$\hat{v}(\hat{x}, \hat{y}, \hat{z}) := v(x, y, z).$$

Now, let χ be a smooth cutoff function on $\hat{T}$ such that $\chi = 0$ in a neighborhood of the edge $\hat{e} := \hat{x}_0 \hat{x}_1$ and $= 1$ at every other node of $\hat{T}$. Let $\rho_{\hat{v}}$ be the distance from $(\hat{x}, \hat{y}, \hat{z})$ to $\hat{x}_0$. Then, by (36),

$$(45) \qquad \kappa_{ev}^n \rho_{\hat{v}}(\hat{x}, \hat{y}, \hat{z}) \lesssim \rho_v(x, y, z) \lesssim \kappa_v^n \rho_{\hat{v}}(\hat{x}, \hat{y}, \hat{z}),$$

and $\kappa_{ev}^n \rho_{\hat{e}}(\hat{x}, \hat{y}, \hat{z}) = \rho_e(x, y, z)$. Let $\hat{u}_I$ be the interpolation of $\hat{u}$ on the reference tetrahedron $\hat{T}$. Since $\chi \hat{u} = 0$ in the neighborhood of $\hat{e}$, $(\chi \hat{u})_I = \hat{u}_I$ and

$$(46) \qquad |\chi \hat{u}|_{H^{m+1}(\hat{T})} \leq C \sum_{|\alpha_\perp|+\alpha_3 \leq m+1} \|\rho_{\hat{e}}^{|\alpha_\perp|-1-a_e} \rho_{\hat{v}}^{\alpha_3 - a_V + a_e} \partial^{\alpha_\perp} \partial_{\hat{z}}^{\alpha_3} \hat{u}\|^2_{L^2(\hat{T})}.$$

Note that by (37), $a_V \geq a_{ev}$. Define $\hat{w} := \hat{u} - \chi \hat{u}$. Then, by the usual interpolation error estimate, $\rho_{\hat{e}} \lesssim \rho_{\hat{v}}$, and (46), we have

$$
\begin{aligned}
|\hat{u} - \hat{u}_I|_{H^1(\hat{T})} &= |\hat{w} + \chi \hat{u} - \hat{u}_I|_{H^1(\hat{T})} \leq |\hat{w}|_{H^1(\hat{T})} + |\chi \hat{u} - \hat{u}_I|_{H^1(\hat{T})} \\
&= |\hat{w}|_{H^1(\hat{T})} + |\chi \hat{u} - (\chi \hat{u})_I|_{H^1(\hat{T})} \leq C(\|\hat{u}\|_{H^1(\hat{T})} + |\chi \hat{u}|_{H^{m+1}(\hat{T})}), \\
(47) \qquad &\leq C \sum_{|\alpha_\perp|+\alpha_3 \leq m+1} \|\rho_{\hat{e}}^{|\alpha_\perp|-1-a_e} \rho_{\hat{v}}^{\alpha_3 - a_V + a_e} \partial^{\alpha_\perp} \partial_{\hat{z}}^{\alpha_3} \hat{u}\|^2_{L^2(\hat{T})},
\end{aligned}
$$

where C depends on m and, through χ, the nodes on $\hat{T}$. Then, using (47), the scaling argument based on (36), and the relation $\rho_{\hat{e}}(\hat{x}, \hat{y}, \hat{z}) = \kappa_{ev}^{-n} \rho_e(x, y, z)$, we have

$$
\begin{aligned}
\|\partial_x(u - u_I)\|^2_{L^2(L_{ev,n})} &\leq C\kappa_v^n \left(\|\partial_{\hat{x}}(\hat{u} - \hat{u}_I)\|^2_{L^2(\hat{T})} + \|\partial_{\hat{z}}(\hat{u} - \hat{u}_I)\|^2_{L^2(\hat{T})} \right) \\
&\leq C\kappa_v^n \sum_{|\alpha_\perp|+\alpha_3 \leq m+1} \|\rho_{\hat{v}}^{\alpha_3 - a_V + a_e} \rho_{\hat{e}}^{|\alpha_\perp|-1-a_e} \partial^{\alpha_\perp} \partial_{\hat{z}}^{\alpha_3} \hat{u}\|^2_{L^2(\hat{T})} \\
&\leq C \sum_{|\alpha_\perp|+\alpha_3 \leq m+1} \kappa_v^{2n\alpha_3} \kappa_{ev}^{2na_e} \|\rho_{\hat{v}}^{\alpha_3 - a_V + a_e} \rho_e^{|\alpha_\perp|-1-a_e} \partial^{\alpha_\perp} \partial_z^{\alpha_3} u\|^2_{L^2(L_{ev,n})} \\
(48) \qquad &\leq C2^{-2mn} \sum_{|\alpha_\perp|+\alpha_3 \leq m+1} 2^{2nm} \kappa_v^{2n\alpha_3} \kappa_{ev}^{2na_e} \|\rho_{\hat{v}}^{\alpha_3 - a_V + a_e} \rho_e^{|\alpha_\perp|-1-a_e} \partial^{\alpha_\perp} \partial_z^{\alpha_3} u\|^2_{L^2(L_{ev,n})}.
\end{aligned}
$$

Then, we consider the following cases.

(I) $(\alpha_3 \leq a_v)$. By (11), (45), $a_V \geq a_v$, and $\alpha_3 - a_v \leq 0$, we have

$$
\begin{aligned}
2^{nm} \kappa_v^{n\alpha_3} \kappa_{ev}^{na_e} \rho_{\hat{v}}^{\alpha_3 - a_V + a_e} &= \kappa_v^{n(\alpha_3 - a_v)} \rho_{\hat{v}}^{\alpha_3 - a_v} \kappa_{ev}^{na_e} \rho_{\hat{v}}^{a_e} \rho_{\hat{v}}^{a_v - a_V} \\
(49) \qquad &\lesssim \rho_v^{\alpha_3 - a_v + a_e} \rho_{\hat{v}}^{a_v - a_V} \lesssim \rho_v^{\alpha_3 - a_V + a_e}.
\end{aligned}
$$

(II) $((1 - a_v^{-1} a_{ev})(m + 1) < \alpha_3 \leq m + 1)$. Following the calculation in (40), by (13) and (45), we have

$$
\begin{aligned}
2^{nm} \kappa_v^{n\alpha_3} \kappa_{ev}^{na_e} \rho_{\hat{v}}^{\alpha_3 - a_V + a_e} &\leq 2^{nm} \kappa_{ev}^{n(\alpha_3 - a_V + a_{ev})} \kappa_{ev}^{na_e} \rho_{\hat{v}}^{\alpha_3 - a_V + a_e} \\
(50) \qquad &= \kappa_{ev}^{n(\alpha_3 - a_V)} \kappa_{ev}^{na_e} \rho_{\hat{v}}^{\alpha_3 - a_V + a_e} \lesssim \rho_v^{\alpha_3 - a_V + a_e}.
\end{aligned}
$$

(III) $(a_v < \alpha_3 \leq (1 - a_v^{-1} a_{ev})(m+1).)$ If $a_{ev} = a_v$, we have $(1 - a_v^{-1} a_{ev})(m+1) = 0$, and therefore such α_3 does not exist. Thus, we only need to consider the case

$a_{ev} < a_v$. Note that $\alpha_3 - a_V + a_{ev} \leq 0$ and $a_{ev} \leq a_e$. Therefore, by (13) and (45), we have

$$2^{nm}\kappa_v^{n\alpha_3}\kappa_{ev}^{na_e}\rho_{\hat{v}}^{\alpha_3-a_V+a_e} = \kappa_v^{n\alpha_3}\kappa_{ev}^{n(a_e-a_{ev})}\rho_{\hat{v}}^{\alpha_3-a_V+a_e}$$

$$(51) \qquad \leq \kappa_v^{n(\alpha_3-a_V+a_{ev})}\rho_{\hat{v}}^{\alpha_3-a_V+a_e}\kappa_{ev}^{n(a_e-a_{ev})}\rho_{\hat{v}}^{a_e-a_{ev}} \lesssim \rho_v^{\alpha_3-a_V+a_e}.$$

Therefore, by (48)–(51), we conclude

$$\|\partial_x(u-u_I)\|^2_{L^2(L_{ev,n})}$$

$$(52) \qquad \leq Ch^{2m} \sum_{|\alpha_\perp|+\alpha_3\leq m+1} \|\rho_v^{\alpha_3-a_V+a_e}\rho_e^{|\alpha_\perp|-1-a_e}\partial^{\alpha_\perp}\partial_z^{\alpha_3}u\|^2_{L^2(L_{ev,n})}.$$

A similar error estimate in the y-direction leads to

$$\|\partial_y(u-u_I)\|^2_{L^2(L_{ev,n})}$$

$$(53) \qquad \leq Ch^{2m} \sum_{|\alpha_\perp|+\alpha_3\leq m+1} \|\rho_v^{\alpha_3-a_V+a_e}\rho_e^{|\alpha_\perp|-1-a_e}\partial^{\alpha_\perp}\partial_z^{\alpha_3}u\|^2_{L^2(L_{ev,n})}.$$

In the z-direction, using (47), $\kappa_v \geq \kappa_{ev}$, the scaling argument based on (36), (12), and (49)–(51), we have

$$\|\partial_z(u-u_I)\|^2_{L^2(L_{ev,n})} = \kappa_v^{-n}\kappa_{ev}^{2n}\|\partial_{\hat{z}}(\hat{u}-\hat{u}_I)\|^2_{L^2(\hat{T})}$$

$$\leq C\kappa_v^{-n}\kappa_{ev}^{2n} \sum_{|\alpha_\perp|+\alpha_3\leq m+1} \|\rho_{\hat{v}}^{\alpha_3-a_V+a_e}\rho_{\hat{e}}^{|\alpha_\perp|-1-a_e}\partial^{\alpha_\perp}\partial_{\hat{z}}^{\alpha_3}\hat{u}\|^2_{L^2(\hat{T})}$$

$$\leq C \sum_{|\alpha_\perp|+\alpha_3\leq m+1} \kappa_v^{2n(\alpha_3-1)}\kappa_{ev}^{2n(1+a_e)}\|\rho_{\hat{v}}^{\alpha_3-a_V+a_e}\rho_e^{|\alpha_\perp|-1-a_e}\partial^{\alpha_\perp}\partial_z^{\alpha_3}u\|^2_{L^2(L_{ev,n})}$$

$$\leq C2^{-2mn} \sum_{|\alpha_\perp|+\alpha_3\leq m+1} 2^{2nm}\kappa_v^{2n\alpha_3}\kappa_{ev}^{2na_e}\|\rho_{\hat{v}}^{\alpha_3-a_V+a_e}\rho_e^{|\alpha_\perp|-1-a_e}\partial^{\alpha_\perp}\partial_z^{\alpha_3}u\|^2_{L^2(L_{ev,n})}$$

$$(54) \qquad \leq Ch^{2m} \sum_{|\alpha_\perp|+\alpha_3\leq m+1} \|\rho_v^{\alpha_3-a_V+a_e}\rho_e^{|\alpha_\perp|-1-a_e}\partial^{\alpha_\perp}\partial_z^{\alpha_3}u\|^2_{L^2(L_{ev,n})}.$$

Then, the proof is completed by (52)–(54). $\qquad\qquad\qquad\qquad\qquad\square$

Then, we formulate our interpolation error analysis for the anisotropic mesh on Ω.

Theorem 4.25. *Recall $\boldsymbol{a}$ in (14). Let a_{V_T} be the parameter (37) associated to the initial ev-tetrahedron $T \in \mathcal{T}_0$. For each vertex $v_\ell \in \mathcal{V}$, let U_ℓ be the union of the initial ev-tetrahedra that have v_ℓ as the singular vertex. Define $\boldsymbol{\sigma} = (\sigma_1, \ldots, \sigma_{N_s})$, such that*

$$\sigma_\ell = \begin{cases} \max_{T\in U_\ell}(a_{V_T}), & 1 \leq \ell \leq N_v; \\ a_\ell, & N_v < \ell \leq N_s. \end{cases}$$

Let $\mathcal{T}_n$ be the triangulation defined in Algorithm 3.2. For $u \in \mathcal{M}^{m+1}_{\boldsymbol{\sigma}+1}(\Omega)$, let u_I be its nodal interpolation on $\mathcal{T}_n$. Then, we have

$$|u-u_I|_{H^1(\Omega)} \leq Ch^m\|u\|_{\mathcal{M}^{m+1}_{\boldsymbol{\sigma}+1}(\Omega)},$$

where $h = 2^{-n}$. In turn, for the finite element solution u_n defined in (8), we have

$$(55) \qquad |u-u_n|_{H^1(\Omega)} \leq C\dim(S_n)^{-m/3}\|u\|_{\mathcal{M}^{m+1}_{\boldsymbol{\sigma}+1}(\Omega)},$$

where $\dim(S_n)$ is the dimension of the finite element space associated with $\mathcal{T}_n$. In both estimates, the constant C depends on $\mathcal{T}_0$ and m, but not on n.

Proof. Note that $\boldsymbol{\sigma} \geq \boldsymbol{a} > \boldsymbol{0}$. Then, the first inequality is the consequence of the definition of the weighted space $\mathcal{M}_{\boldsymbol{\mu}}^m$ and the local interpolation error estimates on different initial tetrahedra: the o-tetrahedra (Lemma 4.1), the v- or v_e-tetrahedra (Corollary 4.5), the e-tetrahedra (Corollary 4.18), and the ev-tetrahedra (Corollary 4.24).

Note that for each refinement, each tetrahedron is decomposed into 8 child tetrahedra. Therefore, the dimension of the finite element space $\dim(S_n) \sim 2^{3n}$. Thus, the second inequality follows from the best approximation property (9) and $h \sim \dim(S_n)^{-1/3}$. $\qquad\square$

Remark 4.26. Given a sufficiently smooth function f in equation (1), the regularity of the solution u (the parameters of the weighted space in the regularity estimates) depends on the geometry of the domain. See (7) for example. Therefore, for a singular solution in the weighted space $u \in \mathcal{M}_{\boldsymbol{\sigma+1}}^{m+1}(\Omega)$, where $\sigma_\ell > 0$ for $1 \leq \ell \leq N_s$, it is sufficient to choose the parameter $\boldsymbol{a}$ that satisfies the condition in Theorem 4.25, in order to recover the optimal convergence rate of the finite element solution.

In particular, for a vertex v and an edge e, let ℓ_v and ℓ_e be the sub-indices in σ_ℓ corresponding to v and e, respectively. Then, to achieve the optimal convergence rate, for the edge e, we can choose the grading parameter

$$(56) \qquad \kappa_e = 2^{-m/a_e}, \qquad \text{for } 0 < a_e \leq \min(m, \sigma_{\ell_e});$$

for the vertex v, we can choose

$$(57) \qquad \kappa_v = 2^{-m/a_v} \qquad \text{for } 0 < a_v \leq m \text{ and}$$
$$a_V = (m+1)(1 - a_v^{-1}a_{ev}) + a_{ev} \leq \sigma_{\ell_v},$$

where a_{ev} is the minimum value of the parameters associated with v and with all the edges touching v (see the definition in (13)).

In addition, using (37), we obtain

$$a_v(a_V - a_v) = (m + 1 - a_v)(a_v - a_{ev}).$$

Since $0 < a_{ev} \leq a_v \leq m$, it can be seen that for ev-tetrahedra, $a_v \leq a_V$. Therefore, by (57), for a given regularity index σ_{ℓ_v} in the weighted space, the optimal value of a_v is usually smaller than that of σ_{ℓ_v}. Intuitively, the additional regularity represented by the difference in the regularity index $\sigma_{\ell_v} - a_v$ is needed to compensate for the lack of the maximum angle condition in the mesh when $a_v > a_{ev}$. In the special case when $a_v = a_{ev}$, we have $a_V = a_v$ and the new ev-tetrahedra generated in each refinement will satisfy the maximum angle condition. Nevertheless, the conditions in (56) and (57) give rise to an optimal range of the grading parameter, for which the proposed finite element solution converges in the optimal rate (55) when $u \in \mathcal{M}_{\boldsymbol{\sigma+1}}^{m+1}(\Omega)$.

5. Numerical results

In this section, using the proposed anisotropic finite element algorithm, we solve the boundary value problem (1) on two model polyhedral domains (the prism and the Fichera corner). These domains represent typical three dimensional vertex-edge solution singularities. It will be evident that the numerical results are aligned with our approximation results presented in Section 4, and thus validate our method. In both numerical tests, we use linear finite elements and let $f = 1$. This is for
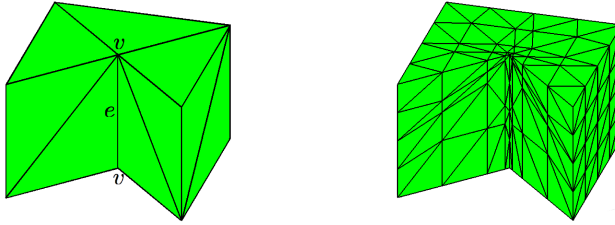
FIGURE 5. The prism domain: the initial triangulation (left) and the mesh after two graded refinements toward the singular edge e ($\kappa_e = 0.2$).

the purpose of simplifying the demonstration of the method. High-order elements solving more complicated equations will be reported in a forthcoming paper.

5.1. **Test I.** [The prism domain] Let T be the triangle with vertices $(0,0), (1,0)$, and $(0.5, 0.5)$, and let the domain be the prism $\Omega := \left((0,1)^2 \setminus T\right) \times (0,1)$ (Figure 5). Then, we solve equation (1) in the variational form (8). Based on the regularity estimates in (6) and (7) the solution is in H^2 in the sub-region of Ω that is away from the edge e where the opening angle is $3\pi/2$. Therefore, a quasi-uniform mesh in such a region will yield a first-order (optimal) convergence for the interpolation error. In the neighborhood of the edge e, by (6) and Table 1 in [19], we have

$$u \in \mathcal{M}_{\boldsymbol{\sigma+1}}^2 \qquad \text{for } \sigma_e < \eta_e = 2/3 \text{ and } \sigma_v < \eta_v = 13/6,$$

where σ_v is the index regarding the regularity of the solution near either of the vertices (endpoints of e) v (see (5)). Then, by (56) and (57), a sufficient condition to attain the optimal convergence rate for the finite element solution is that the mesh parameters satisfy $a_e < 2/3$ and $a_V < 13/6$.

Recall that for linear elements, $m = 1$. Then, using (37), $0 < a_{ev} \leq a_v$, $0 < a_{ev} \leq a_e$, and the fact $a_v, a_e \in (0,1]$, we have

$$a_V = 2 - a_v^{-1}(2 - a_v)a_{ev} \leq 2 - a_{ev} < 2 < 13/6.$$

Therefore, the optimal condition ($a_V < 13/6$) for the vertex v is always satisfied for all the feasible values of a_v and a_e, which implies that the vertex v shall not affect the convergence rate on the anisotropic meshes. Hence, to improve the convergence rate, we only need to implement special edge refinement based on the value of a_e. Thus, in the numerical tests, we choose the parameters for the edge e and for either of the vertices v, such that

$$0 < a_e \leq 1 \qquad \text{and} \qquad a_v = 1.$$

Then, based on Theorem 4.25 and (56), in order to recover the optimal convergence rate for the finite element solution, it suffices to choose $0 < a_e < 2/3$, namely, $0 < \kappa_e = 2^{-1/a_e} < 0.353$. Recall that for $\kappa_{ev} = \kappa_e < 0.5$ and $\kappa_v = 2^{-1/a_v} = 0.5$, the resulting mesh is graded toward the edge e without special refinement for the vertex v. See Figure 5 for such graded meshes when $\kappa_e = 0.2$.

In Table 1, we display the convergence rates of the finite element solution on proposed anisotropic meshes associated with different values of the grading parameter κ_e. Here, j is the level of refinements. Denote by u_j the linear finite element solution on the mesh after j refinements. Since the exact solution is not known,
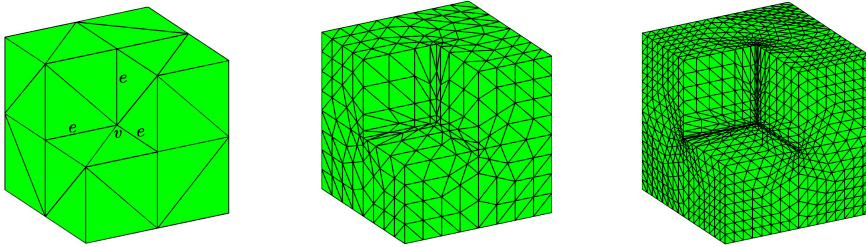
FIGURE 6. The Fichera corner (left to right): the initial mesh, mesh after two refinements, mesh after three refinements ($\kappa_e = \kappa_v = 0.3$).

the convergence rate is computed using the numerical solutions for successive mesh refinements

$$(58) \qquad \text{convergence rate} = \log_2\left(\frac{|u_j - u_{j-1}|_{H^1(\Omega)}}{|u_{j+1} - u_j|_{H^1(\Omega)}}\right).$$

As j increases, the dimension of the discrete system is $O(2^{3j})$. Therefore, the asymptotic convergence rate in (58) is a reasonable indicator of the actual convergence rate for the numerical solution.

It is clear from the table that the first-order convergence rate is obtained for $\kappa_e = 0.1, 0.2, 0.3 < 0.353$, while we lose the optimal convergence rate if $\kappa_e = 0.4, 0.5$, both larger than the critical value 0.353. When $\kappa_e = 0.4$, that is $0.353 < \kappa_e < 0.5$, this choice still leads to an anisotropic mesh graded toward the singular edge, but the grading is insufficient to resolve the edge singularity in the solution, and hence does not lead to the optimal rate of convergence. These results are in strong agreement with the theoretical estimates in Section 4. We also point out that on quasi-uniform meshes ($\kappa_e = 0.5$), the theoretical convergence rate is about $h^{0.66}$. We see in Table 1 that the numerical rate (58) for $\kappa_e = 0.5$ is decreasing and shall approach the theoretical rate 0.66 as j increases.

5.2. **Test II.** [The Fichera corner] Let D_0 be the cube $(-1, 1)^3$ and $D_1 = [0, 1)^3$. Let the domain $\Omega := D_0 \setminus D_1$. Thus, the domain Ω is featured with the Fichera corner at the vertex v and three adjacent edges e with the opening angle $3\pi/2$ (Figure 6). For a sub-region away from these three edges, the solution of equation (1) belongs to H^2, and therefore, a quasi-uniform mesh will lead to the optimal convergence rate for the interpolation error. In the neighborhood of the three

TABLE 1. Convergence rates for the prism domain.

j	$\kappa_e = 0.1$	$\kappa_e = 0.2$	$\kappa_e = 0.3$	$\kappa_e = 0.4$	$\kappa_e = 0.5$
2	0.40	0.46	0.52	0.58	0.60
3	0.75	0.79	0.82	0.84	0.83
4	0.91	0.93	0.94	0.93	0.90
5	0.97	0.98	0.98	0.96	0.91
6	0.99	0.99	0.99	0.97	0.89
7	1.00	1.00	1.00	0.97	0.86

edges, including the Fichera corner, by (6), (7), and Table 1 in [19], the solution satisfies

$$u \in \mathcal{M}^2_{\boldsymbol{\sigma+1}}, \qquad \text{for } \sigma_e < \eta_e = 2/3 \text{ and } \sigma_v < \eta_v \approx 0.954.$$

For the endpoints of the three marked edges, which are not at the Fichera corner, the upper bound of the regularity index is $13/6$. For the same reason as in Test I, these vertices shall not affect the convergence rate for feasible mesh parameters. Then, by Theorem 4.25, the sufficient condition to attain the optimal convergence rate for the finite element solution is that the mesh parameters give rise to $a_e < 2/3$ for the three marked edges and $a_V < 0.954$ for the vertex v. There are many possible values of a_e and a_v that fulfill this requirement. To illustrate our method, in Table 2, we list the convergence rates of the finite element solutions on anisotropic meshes with $\kappa_e = \kappa_v = 0.3$ (accordingly, $a_e = a_v \approx 0.576$) and on quasi-uniform meshes, namely $\kappa_e = \kappa_v = 0.5$ (accordingly, $a_e = a_v = 1$). The rates are computed using numerical solutions as in (58). The finest mesh ($j = 8$) in the numerical tests consists of about 5.9×10^8 tetrahedra, which results in a system of over 10^8 linear equations.

In the case $\kappa_e = \kappa_v = 0.3$, by (37), we have $a_e \approx 0.576 < 2/3$ and $a_V = a_v \approx 0.576 < 0.954$. Therefore, by Theorem 4.25, (56), and (57), we expect to obtain the first-order optimal convergence rate in the finite element approximation. As for the quasi-uniform mesh ($\kappa_e = \kappa_v = 0.5$), since the solution is not globally in H^2, by (10), we expect a sub-optimal convergence rate. It is clear that the numerical results in Table 2 validate this theoretical prediction and hence verify the theory.

TABLE 2. Convergence rates for the Fichera corner.

j	$\kappa_v = 0.3 \quad \kappa_e = 0.3$	$\kappa_v = 0.5 \quad \kappa_e = 0.5$
2	0.64	0.68
3	0.84	0.82
4	0.94	0.86
5	0.97	0.86
6	0.99	0.83
7	0.99	0.80

References

[1] T. Apel, *Anisotropic finite elements: local estimates and applications*, Advances in Numerical Mathematics, B. G. Teubner, Stuttgart, 1999. MR1716824

[2] Th. Apel and B. Heinrich, *Mesh refinement and windowing near edges for some elliptic problem*, SIAM J. Numer. Anal. **31** (1994), no. 3, 695–708, DOI 10.1137/0731037. MR1275108

[3] T. Apel and S. Nicaise, *The finite element method with anisotropic mesh grading for elliptic problems in domains with corners and edges*, Math. Methods Appl. Sci. **21** (1998), no. 6, 519–549, DOI 10.1002/(SICI)1099-1476(199804)21:6⟨519::AID-MMA962⟩3.3.CO;2-I. MR1615426

[4] T. Apel, S. Nicaise, and J. Schöberl, *Finite element methods with anisotropic meshes near edges*, Finite Element Methods (Jyväskylä, 2000), GAKUTO Internat. Ser. Math. Sci. Appl., vol. 15, Gakkōtosho, Tokyo, 2001, pp. 1–8. MR1896262

[5] T. Apel, A.-M. Sändig, and J. R. Whiteman, *Graded mesh refinement and error estimates for finite element solutions of elliptic boundary value problems in non-smooth domains*, Math. Methods Appl. Sci. **19** (1996), no. 1, 63–85, DOI 10.1002/(SICI)1099-1476(19960110)19:1⟨63::AID-MMA764⟩3.0.CO;2-S. MR1365264

[6] T. Apel and J. Schöberl, *Multigrid methods for anisotropic edge refinement*, SIAM J. Numer. Anal. **40** (2002), no. 5, 1993–2006, DOI 10.1137/S0036142900375414. MR1950630

[7] I. Babuška and A. K. Aziz, *On the angle condition in the finite element method*, SIAM J. Numer. Anal. **13** (1976), no. 2, 214–226, DOI 10.1137/0713021. MR0455462

[8] I. Babuška, R. B. Kellogg, and J. Pitkäranta, *Direct and inverse error estimates for finite elements with mesh refinements*, Numer. Math. **33** (1979), no. 4, 447–471, DOI 10.1007/BF01399326. MR553353

[9] C. Bacuta, H. Li, and V. Nistor, *Anisotropic graded meshes and quasi-optimal rates of convergence for the FEM on polyhedral domains in 3D*. In CCOMAS 2012 - European Congress on Computational Methods in Applied Sciences and Engineering, e-Book Full Papers, pages 9003–9014. 2012.

[10] C. Bacuta, V. Nistor, and L. T. Zikatanov, *Improving the rate of convergence of high-order finite elements on polyhedra. I. A priori estimates*, Numer. Funct. Anal. Optim. **26** (2005), no. 6, 613–639, DOI 10.1080/01630560500377295. MR2187917

[11] C. Bacuta, V. Nistor, and L. T. Zikatanov, *Improving the rate of convergence of high-order finite elements on polyhedra. II. Mesh refinements and interpolation*, Numer. Funct. Anal. Optim. **28** (2007), no. 7-8, 775–824, DOI 10.1080/01630560701493263. MR2347683

[12] C. Băcuţă, V. Nistor, and L. T. Zikatanov, *Improving the rate of convergence of 'high order finite elements' on polygons and domains with cusps*, Numer. Math. **100** (2005), no. 2, 165–184, DOI 10.1007/s00211-005-0588-3. MR2135780

[13] J. Bey, *Tetrahedral grid refinement*, Computing **55** (1995), no. 4, 355–378, DOI 10.1007/BF02238487. MR1370107

[14] S. C. Brenner and L. R. Scott, *The Mathematical Theory of Finite Element Methods*, 2nd ed., Texts in Applied Mathematics, vol. 15, Springer-Verlag, New York, 2002. MR1894376

[15] S. C. Brenner, J. Cui, and L.-Y. Sung, *Multigrid methods for the symmetric interior penalty method on graded meshes*, Numer. Linear Algebra Appl. **16** (2009), no. 6, 481–501, DOI 10.1002/nla.630. MR2522959

[16] A. Buffa, M. Costabel, and M. Dauge, *Anisotropic regularity results for Laplace and Maxwell operators in a polyhedron*, C. R. Math. Acad. Sci. Paris **336** (2003), no. 7, 565–570, DOI 10.1016/S1631-073X(03)00138-9. MR1981469

[17] P. G. Ciarlet, *The Finite Element Method for Elliptic Problems,* Studies in Mathematics and its Applications, Vol. 4, North-Holland Publishing Co., Amsterdam-New York-Oxford, 1978. MR0520174

[18] M. Costabel and M. Dauge, *Weighted regularization of Maxwell equations in polyhedral domains. A rehabilitation of nodal finite elements*, Numer. Math. **93** (2002), no. 2, 239–277, DOI 10.1007/s002110100388. MR1941397

[19] M. Costabel, M. Dauge, and S. Nicaise, *Weighted analytic regularity in polyhedra*, Comput. Math. Appl. **67** (2014), no. 4, 807–817, DOI 10.1016/j.camwa.2013.03.006. MR3163880

[20] M. Costabel, M. Dauge, and C. Schwab, *Exponential convergence of hp-FEM for Maxwell equations with weighted regularization in polygonal domains*, Math. Models Methods Appl. Sci. **15** (2005), no. 4, 575–622, DOI 10.1142/S0218202505000480. MR2137526

[21] M. Dauge, *Elliptic Boundary Value Problems on Corner Domains*: Smoothness and Asymptotics of Solutions, Lecture Notes in Mathematics, vol. 1341, Springer-Verlag, Berlin, 1988. MR961439

[22] C. De Coster and S. Nicaise, *Singular behavior of the solution of the Helmholtz equation in weighted L^p-Sobolev spaces*, Adv. Differential Equations **16** (2011), no. 1-2, 165–198. MR2766898

[23] L. C. Evans, *Partial Differential Equations*, Graduate Studies in Mathematics, vol. 19, American Mathematical Society, Providence, RI, 1998. MR1625845

[24] M. Farhloul, S. Nicaise, and L. Paquet, *Some mixed finite element methods on anisotropic meshes*, M2AN Math. Model. Numer. Anal. **35** (2001), no. 5, 907–920, DOI 10.1051/m2an:2001142. MR1866274

[25] R. Fritzsch. *Optimale Finite-Elemente-Approximationen für Funktionen mit Singularitäten*. 1990. Thesis (Ph.D.)–TU Dresden.

[26] P. Grisvard, *Elliptic Problems in Nonsmooth Domains*, Monographs and Studies in Mathematics, vol. 24, Pitman (Advanced Publishing Program), Boston, MA, 1985. MR775683

[27] B. Guo and C. Schwab, *Analytic regularity of Stokes flow on polygonal domains in count-ably weighted Sobolev spaces*, J. Comput. Appl. Math. **190** (2006), no. 1-2, 487–519, DOI 10.1016/j.cam.2005.02.018. MR2209521

[28] E. Hunsicker, H. Li, V. Nistor, and V. Uski, *Analysis of Schrödinger operators with inverse square potentials I: regularity results in 3D*, Bull. Math. Soc. Sci. Math. Roumanie (N.S.) **55(103)** (2012), no. 2, 157–178. MR3075332

[29] V. A. Kondratʹev, *Boundary value problems for elliptic equations in domains with conical or angular points* (Russian), Trudy Moskov. Mat. Obšč. **16** (1967), 209–292. MR0226187

[30] V. A. Kozlov, V. G. Mazʹya, and J. Rossmann, *Spectral Problems Associated With Corner Singularities of Solutions to Elliptic Equations*, Mathematical Surveys and Monographs, vol. 85, American Mathematical Society, Providence, RI, 2001. MR1788991

[31] H. Li, A. Mazzucato, and V. Nistor, *Analysis of the finite element method for transmission/mixed boundary value problems on general polygonal domains*, Electron. Trans. Numer. Anal. **37** (2010), 41–69. MR2777235

[32] J.-L. Lions and E. Magenes, *Non-homogeneous Boundary Value Problems and Applications. Vol. I*, Springer-Verlag, New York-Heidelberg, 1972. Band 181. MR0350177

[33] J. M.-S. Lubuma and S. Nicaise, *Dirichlet problems in polyhedral domains. II. Approximation by FEM and BEM*, J. Comput. Appl. Math. **61** (1995), no. 1, 13–27, DOI 10.1016/0377-0427(94)00050-B. MR1358044

[34] V. Maz'ya and J. Rossmann, *Elliptic Equations in Polyhedral Domains*, Mathematical Surveys and Monographs, vol. 162, American Mathematical Society, Providence, RI, 2010. MR2641539

[35] S. Nicaise, *Polygonal interface problems*, Methoden und Verfahren der Mathematischen Physik [Methods and Procedures in Mathematical Physics], vol. 39, Verlag Peter D. Lang, Frankfurt am Main, 1993. MR1236228

[36] L. A. Oganesjan, V. Ja. Rivkind, and L. A. Ruhovec, *Variational-difference methods for the solution of elliptic equations. I*, Differencialʹnye Uravnenija i Primenen.—Trudy Sem. Processy **Vyp. 5** (1973), 3–389, 391. MR0478669

[37] G. Raugel, *Résolution numérique par une méthode d'éléments finis du problème de Dirichlet pour le laplacien dans un polygone*, C. R. Acad. Sci. Paris Sér. A-B **286** (1978), no. 18, A791–A794. MR497667

[38] D. Schötzau, C. Schwab, and T. P. Wihler, *hp-dGFEM for second-order mixed elliptic problems in polyhedra*, Math. Comp. **85** (2016), no. 299, 1051–1083, DOI 10.1090/mcom/3062. MR3454358

[39] L. B. Wahlbin, *On the sharpness of certain local estimates for H^1 projections into finite element spaces: influence of a re-entrant corner*, Math. Comp. **42** (1984), no. 165, 1–8, DOI 10.2307/2007556. MR725981

DEPARTMENT OF MATHEMATICS, WAYNE STATE UNIVERSITY, DETROIT, MICHIGAN 48202
E-mail address: li@wayne.edu